X-615-69-78
PREPRINT

NASA TM X-63485

THE REDUCTION OF TOPSIDE IONOGRAMS TO ELECTRON DENSITY PROFILES

J. E. JACKSON

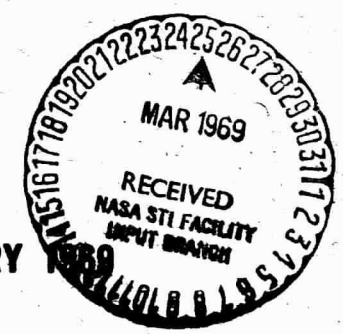

FEBRUARY 1969

GSFC
GODDARD SPACE FLIGHT CENTER
GREENBELT, MARYLAND

THE REDUCTION OF TOPSIDE IONOGRAMS TO ELECTRON DENSITY PROFILES

by

J. E. JACKSON

NASA/GODDARD SPACE FLIGHT CENTER
GREENBELT, MARYLAND 20771

FEBRUARY 25, 1969

To be published in the IEEE June 1969 special issue on the Alouette-ISIS program.

TABLE OF CONTENTS

THE REDUCTION OF TOPSIDE IONOGRAMS TO ELECTRON DENSITY PROFILES

by

John E. Jackson
Laboratory for Space Sciences
NASA Goddard Space Flight Center
Greenbelt, Maryland

ABSTRACT

The basic principles of the ionosonde technique are reviewed with special emphasis given to the satellite version of this technique (topside soundings). It is shown that the lamination method (developed initially for the analysis of ionograms obtained with ground-based ionosondes) can be used to calculate the electron density N vs. true height h in the topside ionosphere provided a number of refinements are introduced. These refinements are required because the extraordinary wave data has to be used to obtain N(h) profiles from topside ionograms, and because these data are very sensitive to the magnetic field variation over the great altitude range of topside soundings (typically one order of magnitude greater than for ground-based soundings). A complete procedure for analyzing topside ionograms, based upon a parabolic-in-log N lamination method is presented which incorporates the actual values of the earth magnetic field at all heights, a change in variable which renders the group path integrand finite at the reflection point,

(and varying sufficiently slowly elsewhere to be calculated very accurately with a 3-point Gaussian integration technique), and iteration until successive calculations agree to within 0.01 km. A procedure was also developed to insure and accelerate the convergence of the iteration process. The importance of each refinement is discussed and illustrated quantitatively. It is shown that this new N(h) reduction technique can, in theory, yield topside electron density profiles with an altitude accuracy of a few kilometers over a 3000 to 400 km altitude range. This theoretical accuracy can be achieved using typically ten to twenty data points per ionogram. In actual practice the errors in the N(h) profiles arise primarily from the limited resolution of the ionograms, calibration inaccuracies, and deviations from vertical propagation. The actual accuracy of topside N(h) profiles is discussed in a companion paper (Jackson, same I.E.E.E. issue).

THE REDUCTION OF TOPSIDE IONOGRAMS TO ELECTRON DENSITY PROFILES

by

J. E. JACKSON

I. INTRODUCTION

Most of our knowledge concerning the distribution of electrons in the ionosphere as a function of position and time has come from ionospheric sounders (ionosondes) located either on the ground or in satellites. Ground-based soundings provide the electron density N as a function of altitude h below the altitude of maximum electron density hmaxF2, (typically at 300 km) and topside soundings provide the N(h) data from the topside sounder altitude down to hmaxF2. Other experimental configurations which have been used include sounders in aircraft and in rockets. Thus sounders can be either mobile or geostationary and be located either above or below hmaxF2.

Ionosondes operate on principles similar to those of radar. There are, however, important differences. The ionosonde does not receive echoes from hard targets as is usually the case with radar. The ionosonde target is a plasma, whose reflection properties are highly frequency-dependent. The reflection conditions, which will be discussed later, are such that 1) the ionosonde must utilize frequencies lower than those normally used in radar and 2) a large number of sounding frequencies are required in order to investigate the plasma and obtain its electron density distribution. This last requirement is best met with the swept-frequency system which is commonly used in ground-based ionosondes, and which was selected for the Alouette I and Alouette II sounders. Single or multiple fixed-frequency sounders have also been utilized for special applications. For example, the Explorer XX sounder operated at six fixed frequencies (references to this issue to be provided by editors).

In conventional radar applications the round trip time for a reflected signal is readily converted to target distance, since the radar signal travels essentially at the velocity of light in vacuo.

A similar round-trip-time to distance conversion is required in the reduction of the ionosonde data, but in this case the problem is much more difficult. The conversion process must take into consideration the fact that the signal velocity varies continuously while the propagation path is within the ionosphere. In the ionosphere the signal velocity is less than the velocity of light in vacuo resulting in a retardation of the signal. The calculation of this retardation, so that real distances to the point of reflection can be determined, is a subject which has received the attention of ionospheric workers since the earliest days of radio sounding experiments. The techniques used to perform these calculations are based upon the magneto-ionic theory (Budden 1961, Kelso 1964, Ratcliffe 1959). A single reduction technique, however, cannot be used for all the possible experimental configurations, because each presents its own special problems. Thus techniques developed during the 1940 and 1950 decades for the reduction of ground-based ionograms were not directly applicable to the analysis of topside ionograms.

For a number of reasons, including practical considerations such as the need for minimizing computation time, a large number of techniques (Radio Science, Oct. 1967) were developed for the reduction of ground-based soundings. The availability of fast computers has led to the adoption of the lamination technique (discussed later) for most of the N(h) work based upon ground-based soundings. In view of its flexibility and accuracy, the lamination technique was also selected for the analysis of topside ionograms. Extensive modifications and refinements had to be incorporated in this technique in order to meet the special requirements of topside N(h) analysis. Much of the present paper is devoted to a discussion of these topics.

The ionogram reduction techniques in common use all assume that the soundings are vertical. This assumption, in general, does not introduce serious errors in the reduction of ground-based soundings. For topside soundings, however, the assumption can lead to large errors in N(h) results. The magnitude of the error due to non-vertical propagation tends to increase with satellite altitude. On Alouette II, for example, the ionograms taken from altitudes above 2000 km are frequently the results of reflections

obtained under conditions of oblique propagation. Oblique propagation is much less of a problem on Alouette I ionograms which corresponds to soundings taken from a nearly constant altitude of 1000 km, or on Alouette II ionograms when the Alouette II altitude is less than 1500 km. Proper care must therefore be exercised in the selection of topside ionograms for N(h) analysis, and when this is done the errors in the derived profiles are usually less than 10 percent. This error estimate is based upon typical results obtained when profiles derived from topside ionograms were compared with profiles obtained simultaneously by other techniques, such as rocket and incoherent backscatter measurements (see paper in this issue "Comparisons between topside and ground-based Soundings" by J. E. Jackson).

Using procedures more elaborate than those employed for vertical soundings, it is often possible to derive reliable N(h) profiles from ionograms obtained under conditions of oblique propagation. For example, consecutive high altitude ionograms often show clear traces corresponding to propagation along magnetic field lines; these traces can be used to compute a series of field aligned profiles from which the N(h) profiles can be derived (Colin, Dufour and Willoughby, this issue). In this case the initial field-aligned profiles are calculated using the same basic methods described here. With more complex reduction techniques (Lockwood, this issue), vertical N(h) profiles can in many cases be obtained from more general (non field-aligned) oblique soundings. These methods, however, are not presently in general use and they are not the subject of this paper.

Although some of the topside ionograms are unsuitable for N(h) analysis, they often provide the basis for investigating various ionospheric phenomena such as partial field-aligned ducts, spread-F, and other irregularities (reference to appropriate papers in special issue). Another important use of ionograms has been for the study of plasma resonances (reference to special issue). The topside sounder is therefore a very versatile tool for ionospheric studies, the N(h) analysis discussed in this paper being only one of the many applications of topside soundings.

II. DISCUSSION OF p'-f DATA ON TOPSIDE IONOGRAMS

The ionograms which will be discussed are those obtained with topside sounders which sweep in frequency from about 0.1 to 20 MHz emitting short pulses at 20 to 60 pulses per second. The received echoes are conventionally displayed in the "ionogram" format (Franklin, et al; Hagg; this issue) in which the time delay between pulses is displayed as a vertical axis, calibrated in terms of apparent range p'. This calibration assumes that the wave travels at the velocity, c, of light in vacuo. In general p' is larger than the actual distance to the echoing region because the sounding signal is retarded by the ionosphere. By calculating the extent to which each sounding frequency is retarded, the N(h) profile can be computed. The group velocity V_G of the sounding signal varies as a function of frequency f, electron density, terrestrial magnetic field B and the angle φ between $\vec{B}$ and the direction of propagation. It is the complexity of the V_G function which has made it necessary to develop special techniques for converting ionograms to N(h) profiles.

By definition, the apparent range at a frequency f_1 is one half the measured round-trip time (Δt_1) multiplied by the velocity of light in vacuo. Consequently:

$$p'(f_1) = \frac{c}{2} (\Delta t_1) \qquad (1)$$

The round-trip time is given by:

$$\Delta t_1 = 2 \int_{p_o}^{p_1} \frac{dp}{V_G} \qquad (2)$$

where the integration is along the path taken by the wave, p_o is the position of the sounder and p_1 corresponds to a reflection point for the frequency f_1. Combining equations (1) and (2) gives:

$$p'(f_1) = \int_{p_o}^{p_1} \left(\frac{c}{V_G}\right) dp \qquad (3)$$

In standard magneto-ionic nomenclature the quantity c/V_G is called the group refractive index n'. Equation (3) then becomes:

$$p' = \int_{p_o}^{p_1} n' dp \qquad (4)$$

The behavior of n' is usually described in terms of a parameter X* which is proportional to N/f^2. Although this conventional approach is used later in the text, it is more convenient here to use a V_G - vs - f diagram. A V_G-f diagram is shown in Figure 1 for one set of values of N, B and φ. In spite of broad variations, certain features are common to all V_G-f diagrams. First, there are always three group-velocity curves as indicated on Figure 1. These curves are conventionally called Z, ordinary (O) and extraordinary (X)*. The "ordinary" mode is the only one which would be present in the absence of a magnetic field. Second, there are <u>two</u> values of V_G over most of frequency range for which propagation is possible ($V_G > 0$). They correspond to the two independent modes of propagation that are possible when $B \neq 0$, the ordinary and the extraordinary modes. These two modes are present on the ionograms because a plane polarized wave is transmitted by the sounder and its two circularly polarized components propagate independently at their respective group velocities. The reflection points for the Z, (O) and (X) components are labelled fz, fN, and fx. The plasma frequency fN is a function of N only, whereas fz and fx depend upon both N and B. The apparent ranges for the Z, (O) and (X) traces are related to the true range at any given point by an integral such as the one shown in Equation (3). The V_G function appropriate for the particular mode must of course be used in the integral. The point on the Z curve labelled fzI (fz, infinity) is called the Z-mode cut off and is the maximum frequency at which the Z wave can propagate for the given values of N, B, and φ.

* <u>Note for printer</u>: X and (X) are two different symbols. Perhaps script letters could be used for (X) and also for (O) and Z.

The curves of Fig. 1 were calculated for conditions existing at the satellite when the topside ionogram of Fig. 2 was obtained. Thus, Fig. 1 indicates the frequencies at which fz, fN, and fx would be seen on the ionogram for conditions near the satellite. The letter S is often added to fx and fz as done in Fig. 2 when fx and fz refer to conditions near the satellite. On topside ionograms the Z- mode cut-off fzI occurs at the satellite, resulting in very large Z-wave delays as the sounding frequency approaches fzI, and consequently the fzI phenomenon is exhibited as a maximum range effect for the Z-wave. The complete Z, (O) and (X) traces are of course influenced by the gradual changes in ambient conditions along the propagation path, i.e., by the continuous changes in $V_G(N, B, \varphi, f)$ from the satellite altitude down to the various reflection points. There are other features on the ionogram, such as the resonances occurring at fH (gyrofrequency) and at fT (upper hybrid frequency). A strong resonance is also present on this particular ionogram at the second harmonic of the gyrofrequency (2fH). Plasma resonances are discussed in other papers of this issue (appropriate references from editors). Also visible on Fig. 2 are echoes due to the side-band responses of the transmitted pulse (See Hagg & Hewens, Warnock, this issue). There is one response below the main spectrum and two responses above. These side-bands are very clearly seen on the Z' trace of Fig. 2. This Z' trace is an additional Z trace originating from the plasma resonance (Calvert, 1966).

In principle, electron density profiles can be calculated from either the Z, (O) or (X) traces. Since the three traces are affected quite differently by the ionospheric conditions, the analysis techniques can be checked by comparing results obtained from each of the three traces. The results of such a comparison using the data of Fig 2 are shown in Fig. 3. However, as seen in Fig. 1, the Z-wave is normally cut-off at the satellite and does not penetrate down to the maximum of the F-2 region. Since exceptions to this rule are extremely rare (Jackson, 1967, p. 21), the Z-trace (Colin, this issue) is seldom used for N(h) analysis.

This difficulty, however, is not present on either the (O) or the (X) traces, and either trace can be used to derive an N(h) profile. An analysis based upon the ordinary trace is somewhat simpler, because the reflection density is independent of the magnetic field. A more important consideration, however, is the relative quality of the (O) and (X) data.

In the lower ionosphere (D and E regions), collisions between electrons and neutral particles cause low frequency waves to be attenuated. The absorption is more severe for the (X) mode than for the (O) mode. Consequently on ground-based ionograms the (O) trace is usually more complete and therefore it is the one used in N(h) analysis. The situation is different on topside ionograms. Attenuation due to collisions is negligible; the controlling factors are now the sounder antennas and the fact that reflection at a given density N_R occurs at a higher frequency for the (X) mode than for the (O) mode. For example, if N_R = 1240 el/cc and fH = 1.0 MHz, the (O) ray reflects at f = 0.316 MHz and the (X) ray reflects at f = 1.09 MHz. Although the antennas used in a topside sounder satellite are physically very long, they are electrically short (and hence difficult to match to the transmitter) at the low-frequency end of the sweep. Based upon this consideration alone, transmission at 0.316 MHz would be considerably weaker than at 1.09 MHz. The situation is made even worse because the antennas are immersed in the ionosphere. This situation causes a change in antenna impedance, which is particularly severe near the plasma frequency. The net result is that the low-frequency end of the (O) trace is often missing on topside ionograms, and consequently the (X) trace is normally used for the N(h) analysis.

The preceding qualitative discussion omitted most of the usual formulas. The quantities of interest and the corresponding formulas are listed below. The basic ionospheric parameters which affect radio soundings are:

N = ionospheric electron number density (electrons/cm^3)

B = induction (gauss) of terrestrial magnetic field

φ = angle between $\vec{B}$ and direction of propagation

The plasma frequency fN (ordinary ray reflection point) and the gyrofrequency fH depend only upon one ionospheric parameter as indicated below:

$$fN_{(MHz)}=(8.98\times10^{-3})\sqrt{N} \tag{5}$$

$$fH_{(MHz)}=(2.8)B \tag{6}$$

The upper hybrid frequency fT, the extraordinary wave reflection point fx and the Z wave reflection point fz depend upon both N and B as follows:

$$fT=\sqrt{fN^2+fH^2} \tag{7}$$

$$fx=\frac{fH}{2}+\frac{\sqrt{4fN^2+fH^2}}{2} \tag{8}$$

$$fz=fx-fH \tag{9}$$

From Equation 8 and 9,

$$fN^2=fx(fx-fH)=fxfz = (N/12,400 \text{ if frequencies are in MHz}) \tag{10}$$

The high frequency cut-off (fzI) of the Z-wave depends upon N, B and φ as indicated below:

$$fzI = \sqrt{\frac{fT^2+\sqrt{fT^4-4fN^2fH^2COS^2\varphi}}{2}} \tag{11}$$

Finally, the group velocity V_G (or equivalently the group refractive index $n'=c/V_G$) and consequently also the group path integral $p_1' = \int_{p_0}^{p_1} n'dp$ depend upon not only N, B and φ, but also upon the frequency of the sounding signals.

For the special case in which reflections are vertical, p = h, and $\varphi = 90^o-\theta$, where θ is the magnetic dip. Since vertical propagation is assumed in the subsequent analysis, the group path integral will be written in terms of real heights as follows:

$$p'(f) = \int_{h_0}^{h_R(f)} n'[N(h),\ f, B(h), \theta(h)]\ dh \qquad (12)$$

where:

h = actual height

h_0 = height of sounder (satellite altitude for a topside sounder)

h_R = height at which reflection occurs for frequency f

n' = group index of refraction

The basic problem which must be solved in the N(h) analysis is the inversion of the group path integral, i.e., the conversion of the p'(f) function to the N(h) function. The remainder of this report discusses this conversion for the case of vertical propagation. It should be noted that Equation (12) does not give the function n' in explicit form. The formula for n' is quite complicated, (see appendix A) and is not needed for the present discussion. Tables giving values of n' under a wide range of conditions have been published (Becker, 1960).

III. OUTLINE OF THE LAMINATION CONCEPT

For a given geographic location and a given N(h) distribution, it is a relatively straight forward matter to evaluate the integral shown in Equation (12). For a given frequency f, the density N_R at the reflection point is known from Equation (10), and the integration limit h_R follows immediately from the known N(h) function. The magnetic field parameters are known as a function of altitude. Thus all the required quantities are known in the group height integral of Equation (12). Although the integration cannot in general be performed analytically, it is nevertheless relatively simple, when N(h) is known, to compute p'(f) by a numerical integration technique. The basic problem involved in the analysis of an ionogram is to perform the opposite conversion, namely to derive the N(h) function from a knowledge of the p'(f) function. It is, however, not generally possible to invert analytically the group

height integral. The method used is to find a general model for N(h), with many adjustable parameters, which will satisfy Equation (12) for selected values of the p'(f) function. The number of parameters which can be determined is the same as the number of p'(f) values selected for the analysis. With the lamination technique used in this report the N(h) function is represented by a number of points (N_j, h_j) connected by simple analytic curves. More specifically, in a given height interval (h_{j-1} to h_j), the profile is assumed to be of the form:

$$h = h_{j-1} + F_j(N) \qquad (13)$$

where $F_j(N)$ is a simple analytic function of density and where N_j would be the density at h_j. For the parabolic-in-log N method, the electron density profile is assumed to consist of k laminations as shown in Fig. 4. The first lamination (h_0, h_1) which begins at the satellite height h_0 and extends down to the height h_1, is assumed to be linear-in-log N. All other laminations, such as (h_{j-1}, h_j) between heights h_{j-1} and h_j are assumed to be parabolic-in-log N with continuous slopes at the boundaries. A detailed treatment of the extraordinary trace analysis based upon parabolic-in-log (N) laminations is given in Appendix C. The lamination method, however, is more readily visualized in terms of the following simplified set of conditions.

Assume that 1) the p'(f) function under analysis is the ordinary trace of a topside ionogram; 2) the trace is defined for $fN \leq f \leq fm$, where fN is the plasma frequency at the satellite and fm is the maximum frequency at which (0) reflections are obtained; and 3) the corresponding N(h) profile will be approximated by a succession of linear segments (i.e., within a given lamination h varies linearly with N). The procedure which will be described is such that the laminations are derived from a sequence of (p', f) values selected prior to analysis. In the sequence (p'_j, f_j), f increases monotonically with j and (p'_0, f_0) corresponds to zero range on the (0) trace, i.e., $p'_0 = 0$ and $f_0 = fN$.

For the assumed linear lamination, Equation (13) becomes:

$$h = h_{j-1} + a_j \, (N-N_{j-1}) \tag{14}$$

from which

$$dh = a_j \, dN \tag{15}$$

Writing Equation (12) in terms of the laminations shown in Equation (14) and changing from the variable h to the variable N yields:

$$p'(f_j) = \sum_{i=1}^{i=j} a_i \int_{N_{i-1}}^{N_i} n' \, dN \tag{16}$$

where N_j is the density at which reflection occurs at the frequency f_j, i.e., N_j is given by Equation (10). The right hand of Equation (16) represents an integration over (j) laminations. For the first lamination, i.e., the lamination nearest to the topside sounder:

$$p'(f_1) = a_1 \int_{N_0}^{N_1} n'(N,f_1,B,\theta) \, dN \tag{17}$$

The integral in Equation (17) can be evaluated with adequate accuracy by assuming B and θ to be constants and equal to their values at the satellite. This approximation can be made because the ordinary ray group height integral is not very sensitive to the small variation in B and θ which occurs within the altitude range of a typical lamination. With this assumption, a_1 is completely defined by Equation (17) and from Equation (14) it follows that

$$h_1 = h_0 + a_1 \, (N_1-N_0)$$

where

h_0 = height of the satellite

N_0 = electron density at satellite (given by Equation (10) and letting f = fN at the satellite).

For the second lamination:

$$p'(f_2) = a_1 \int_{N_0}^{N_1} n'(N,f_2,B_0,\theta_0)dN + a_2 \int_{N_1}^{N_2} n'(N,f_2,B_1,\theta_1)dn \qquad (18)$$

where N_2 is related to f_2 by formula (10). It should be noted that the integral associated with a_1 is now for the frequency f_2, and also that the value of B and θ used in the second integral corresponds to the altitude h_1 (which is obviously a more correct estimate of B and θ in the second lamination). Equation (18) yields a_2 since this is the only unknown quantity, and consequently:

$$h_2 = h_1 + a_2 (N_2-N_1)$$

This step-by-step procedure is continued until the entire profile is determined. The relatively simple procedure described above has been used for the analysis of ionograms obtained from ground-based sounders (Jackson 1956). An additional simplification which is permissible in the (0) ray analysis of ground-based soundings is to use constant values of B and θ at a given location, since the ionograms correspond to a relatively small altitude range (typically 100 to 300 km). In topside N(h) analysis, it is usually also permissible to treat θ as a constant (value of θ at the satellite for a given ionogram), but the altitude variation of B must be taken into consideration. The techniques used for the reduction of topside ionograms are basically refinements of the simple lamination concept outlined above. Section IV gives a general discussion of these refinements, and Section V indicates the improvements in accuracy resulting from these refinements.

A more detailed discussion of the N(h) reduction technique is given in Appendices A, B, and C.

IV. DISCUSSION OF THE LAMINATION METHOD

Selection of Data Points

From the preceding discussion of the lamination procedure, it was seen that the number of laminations obtained is determined by the number of p'-f values selected for the ionogram reduction

The choice of p'-f values is not particularly critical, provided these data points are sufficient in number and adequately distributed. Methods developed for the selection of data points take into consideration, not only the computer time required, but also the available scaling facilities. For example, at the Goddard Space Flight Center (GSFC), ionograms are scaled with a graphic digitizer, which yields several hundred p'-f values per ionogram. Since this number of data points is one order of magnitude greater than required for N(h) analysis, the automatic analog-to-digital conversion is followed by a selection process. The selection process is a computer operation, done according to a fixed rule (GSFC criterion) and designed to provide enough data points in all cases (typically 25 points), while avoiding excessive computer time. In many cases the GSFC criterion (Jackson 1967, p. 6 of appendix B) yields more points than necessary, but this slight disadvantage is more than compensated by the simplicity of the system. The GSFC criterion was used to scale the ionograms discussed in this report.

Lamination Model

Closely related to the number of points used in the analysis is the model used in the lamination technique. If a large number of points is used, then the resulting profile will be fairly accurate, even with the simple linear model used in the earlier example. However, the number of numerical integrations required increases as the square of the number of p'-f values used in the calculations. With a more elaborate model fewer points can be used in the calculation with an attending reduction in the computer time required, or a greater accuracy can be achieved using the same number of p'-f points in the calculations. Actually, in the topside ionosphere the electron density profile is represented more accurately by a succession of exponential segments, (Fitzenreiter and Blumle, 1964), i.e., the height increments are almost linear in log N, namely:

$$\Delta h = a_j \, (\ln N - \ln N_{j-1}) \qquad (19)$$

One objection to the linear-in-N or linear-in-log N representation is that the assumed profile has discontinuous derivatives at each of the lamination boundaries. This difficulty is readily overcome by assuming that the height increments are parabolic with continuous slopes at the boundaries. The parabolic-in-log N assumption (Paul and Wright, 1963: Doupnik and Schmerling, 1965) assumes that:

$$\Delta h = a_j \ln N/N_{j-1} + b_j [\ln N/N_{j-1}]^2 \qquad (20)$$

with the slope continuity yielding:

$$a_{j+1} = a_j + 2b_j \ln (N_j/N_{j-1}) \qquad (21)$$

The number of laminations is determined by the number of scaled p'-f points, and the actual values of each p'-f pair determine the end points of the N-h laminations. However, since the analysis yields also the equation of each lamination, it is possible to calculate intermediate N(h) values to the same accuracy as that of the end points. Thus the analysis can yield either densities at fixed heights (such as at multiples of 100 km) or heights for pre-selected values of fixed densities.

Evaluation of the Group Height Integral

The following comments are concerned with the method used for evaluating an integral such as the one shown in Equation (17). There are three types of problems to be considered, the first one involves the parameters used in the integrand, the second one is concerned with the limits of integration, and the third one is the integration technique itself.

In the example given earlier (O-trace, linear laminations) it was assumed that B was constant in each lamination. This yields a fairly accurate value of the height h_1 and consequently of the altitude interval over which the integration is performed. Having determined the parameter a_1, the altitude and the value of B are known for each value of N used in the numerical integration.

Hence the integral can be evaluated again, this time associating a more accurate value of B with each value of N used in the integration. This will yield a slightly different value of a_1 and h_1. The process converges very rapidly and after a couple of iterations there are no further significant changes in the final answer.

The principle of iteration is slightly more complicated when extraordinary data are used in the calculations, since in this case it is not only the integrand which is affected but also the upper integration limit. If Equation (17) referred to a virtual height for the extraordinary ray, then the upper limit of integration N_1 would be given by Equation (10) for the extraordinary trace ($f_1 = f_x$), namely:

$$N_1 = 12{,}400\ f_1\ (f_1 - 2.8B_1)$$

The value of B_1 is not known, and it would have to be initially estimated by letting $B_1 = B_0$. Solving Equation (17) with this assumption would yield a fairly good estimate of h_1 and hence B_1. The procedure could then be repeated, using not only a more accurate value of the integration limit N_1, but also more representative values of B within the integrand. It is natural to anticipate that iteration should be more important for the extraordinary ray than for the ordinary ray. Further discussion of the iteration technique is given in Appendix C.

The final point is concerned with the integration technique. The problem which arises here is the fact that the integrand is infinite at the reflection point. Although it has been known for at least 18 years (Poeverlein, 1951; Shinn, 1951; Jackson, 1956) that this infinity can be removed by means of a suitable change of variable, the importance of this transformation was not fully appreciated until quite recently. Some of the early topside N(h) programs were based upon the assumption that a 16-point Gaussian

integration technique could yield an accurate answer for an integral such as the one appearing in Equation (17). It turns out that this technique is both inefficient and inaccurate. Calculations (see Appendix B) for the (X) wave, longitudinal propagation, and an exponential lamination terminating at the reflection point, show that the numerical integration will be in error by 5.5% using a 7-point Gaussian and by 2.5% using a 16-point Gaussian, whereas the error is less than 0.005% if the same integral is evaluated numerically after making the suggested change of variable and using only a 3-point Gaussian integration technique. Similar results are obtained when the propagation is not longitudinal.

The accuracy of the (O) wave group retardation calculations can also be considerably improved by making a change of variables which keeps the integrand finite. A 3-point Gaussian is not adequate, however, except for low dip angles. As the dip angle is increased from 50 to 85 degrees, the number of points used in the Gaussian integration has to be increased from 3 to 16 in order to maintain an accuracy of better than 0.1%. Table 1 illustrates the errors for typical Gaussian integration and for various values of the magnetic dip angle. The errors shown in Table 1 are for the first lamination of the high density Bauer profile discussed in Section V. The density ratio N_1/N_o for this lamination is 1.05. Using the 3-point Gaussian, the errors are typically three times larger for the 10th lamination (density ratio = 1.18) and five times larger for the 27th lamination (density ratio = 1.26). Comparable results were obtained with the low density Bauer profile discussed in Section V. Similar calculations (for the bottomside ionosphere) by Shinn and Whale (1951) led to the conclusion that their results became inaccurate when the dip angle was equal to or greater than 81 degrees. Becker (1960) did not give data beyond 80 degree dips in his tables. Present computer accuracies and integration techniques yield satisfactory results up to at least 87 degrees.

DIP	3-POINT	7-POINT	12-POINT	16-POINT
0-50°	----	----	----	----
70°	0.1%	0.01%	----	----
80°	1.1%	0.1%	----	----
85°	5.5%	0.5%	0.1%	----
87°	17.5%	1.5%	0.3%	0.1% (est.)
89°	200%	10%	1.5%	0.5% (est.)

Table 1 - Error in O-ray group height integrals for a lamination terminating at the reflection point. Blanks in the above table indicate that errors are much less than 0.1 percent.

The integrand is kept finite at the reflection point by means of the following change of variables:

$$t^2 = 1-X \qquad \text{for the ordinary ray}$$

$$t^2 = 1-X/(1-Y_R) \qquad \text{for the extraordinary ray}$$

where:

$$X = 80.6\ N/f^2$$

$$Y_R = \text{value of Y at reflection point}$$

$$Y = fH/f$$

In the above commonly used expression for X, N is in electrons/cc and f is in kHz.

The change of variable eliminates the infinity at the reflection point for the following reason. The formulas giving n' near a given reflection point (Jackson 1967, Appendix A, p. A7 and A8) are of the form:

$$n' = K/\sqrt{1 - kN}$$

where K and k are constants appropriate for the propagation mode used. By letting $t^2 = 1-kN$, a typical group height integral such as the one shown in Equation (16) becomes:

$$\int_{N_{i-1}}^{N_i} n'dN = -\frac{2}{k}\int_{t_{i-1}}^{t_i} n't\,dt$$

At the reflection point, the integrand n't is finite since:

$$n't = n\sqrt{1-kN} = K$$

V. DISCUSSION OF p'-f TO N(h) CONVERSION ERRORS

Accurate analysis of topside ionograms require special care in a number of areas, such as the selection of data points, the choice of lamination technique, the use of iteration in the calculations, and the method used for the numerical evaluation of the group height integral. The importance of these considerations can be tested with ionograms corresponding to a known electron density distribution. The first test is to determine how well the topside p'-f reduction technique (with all its present refinements) will reproduce the known N(h) profile. In subsequent tests various refinements are omitted and the resulting errors determined.

The reference N(h) profiles (Fig. 5) used in the error study were two theoretical topside N(h) distributions based upon a ternary ion mixture in diffusive equilibrium (Bauer, 1962). It is assumed that the ionograms were obtained from an altitude of 3000 km (which corresponds to the apogee of Alouette II) and that the local electron densities were respectively 1000 el/cc for the low density profile and 5000 el/cc for the high density profile. For this theoretical situation it was assumed that the gyro-frequency at the satellite was 0.38 MHz and that the magnetic field varied with altitude according to an inverse cube law. The corresponding ionograms (X-traces) are shown in Fig. 6 and 7. To compute the ionograms, the profiles were divided into linear-in-log N laminations 5 km thick. The scaling criterion mentioned earlier was applied to the set of 520 p'-f values

thus obtained, yielding the points (open and solid) shown on the ionograms. The solid points illustrate a less detailed scaling in which approximately half of the data points would be eliminated. Based upon additional p'-f calculations, using 10 km and 20 km laminations, it was concluded that the errors in the p'-f data (obtained with the 5 km laminations) were less than 1 km.

The normal GSFC procedure for reducing the (X) trace is to use the data points given by the scaling criterion, to assume laminations parabolic-in-log N, to iterate the height calculation for each new lamination until the results converge to within 0.01 km, and to integrate with a 3-point Gaussian after making the change of variable $t^2 = 1-X/(1-Y_R)$. Using this procedure, the maximum error in altitude is about 1 km for both the high-density and the low-density profiles. This error is small compared to the errors due to uncertainties in the scaling of ionograms. Even on excellent ionograms the scaling error on the virtual heights is at least 5 km. Hence the recommended calculation procedures will not contribute significantly to the total error in the ionogram reduction process. Furthermore, even if scaling errors could be made negligible, a maximum error of 1 km would not be significant, particularly on a profile extending from 400 to 3000 km. Deviations from the recommended procedure, however, can sometimes introduce large errors as will be shown in the following discussion.

1. Selection of data points

Satisfactory accuracy in the N(h) reduction of topside ionograms can in general be achieved using 10 to 20 well selected p'-f values. For reasons discussed earlier, the GSFC criterion will in general yield a number of data points slightly greater than necessary. More importantly the criterion will very seldom yield an insufficient number of points. For example, on the low density profile the criterion yields 24 data points and a maximum error in altitude of 1 km. If the calculations are done with only 13 data points the maximum error becomes equal to 6 km, which is still relatively small. The error for these two cases is shown as a function of altitude on

Fig. 8 and 9 (graphs labelled: parabolic). These results indicate that the number of points given by the scaling criterion is not marginal, since it is possible to eliminate approximately half of these points and still achieve a satisfactory accuracy.

2. Choice of lamination model

Performing the same calculations with the low density profile, but assuming laminations linear in log N, yields a maximum error of 20 km for the 24 point analysis, and 50 km for the 13 point analysis. The error for the linear lamination calculation is also shown in Fig. 8 and 9 (graph labelled: linear). Similar results were obtained for the high density profile. In this case the linear-in-log N lamination yielded a maximum error in altitude of 15 km using the 28 points provided by the scaling criterion, and the maximum error was 40 km when only 15 points were used in the calculations.

This leads to the conclusion that the parabolic lamination method yields results about 10 times more accurate than those obtained with the linear lamination method. Furthermore, the use of the linear lamination causes the profile to be too high.

3. Importance of iteration

From the discussion in Section IV, it is seen that the concept of iteration applies only to the last lamination, i.e., the lamination nearest to the reflection point. Iteration is important only when the evaluation of this lamination is very sensitive to the height variation of the magnetic field. Thus iteration is particularly important for the analysis of the (X) trace when the corresponding electron densities are very low. Errors which can arise in the absence of iteration are shown in Fig. 10 for the theoretical ionogram of Fig. 6 (based upon the high density profile) and for two lamination models. It is seen that the largest errors occur when the parabolic-in-log N laminations are used. The error curve for the parabolic lamination also exhibits large oscillations since an error in one lamination provides both an incorrect starting point and an incorrect initial slope for the next lamination. Repeating the above calculations with the ionogram

for the low electron density profile, leads to errors so large that the resulting profile is no longer monotonic.

The parabolic-in-log N lamination leads to much greater accuracy, however, when iteration is performed (see Fig. 8 and 9). The linear-in-log N lamination provides a much better initial estimate of the lamination thickness and this estimate is used as the starting point for the parabolic technique. This procedure speeds up the convergence process (the 0.01 km convergence criterion being usually satisfied after 3 iterations) and also helps in preventing the parabolic calculation from going astray.

4. Choice of integration technique

To show the importance of the change of variable in performing the integration, the ionogram for the low density profile was analyzed using the parabolic-in-log N lamination technique, iterating until Δh was less than 0.01 km, but omitting the change of variable. The integration was performed with both a 7-point Gaussian and a 16-point Gaussian. The error is shown as a function of altitude in Fig. 11. Even with a 16-point Gaussian an error of 22 km can take place. The errors are such as to make the profile appear too low.

5. Comparable observations using actual Alouette II ionograms

An error analysis was made on two Alouette II ionograms, taken from altitudes of 958 and 2873 km, with local electron densities of 2.3×10^4 and 1.3×10^3 respectively. The analysis used a refined magnetic field model (Daniels and Cain, September 1965 model), and it was assumed arbitrarily that the parabolic-in-log N techniques would yield a correct answer. The results, shown in Fig 12, indicate that the errors found with the high altitude ionogram were comparable to the errors found with the low density Bauer profile. Curve C for the high altitude case (Fig. 12) was smoothed; prior to smoothing it was similar to the corresponding curve on Fig. 10. Although a 7-point Gaussian integration was used to calculate curves C, the same results would be obtained with a 3-point Gaussian integration. It is also seen that the

errors are much smaller for the low altitude ionogram. In particular, iteration is not nearly as important for a low altitude ionogram as for a high altitude ionogram.

Errors obtained when an inverse cube law is used (based upon the correct value of B at h_s) have been investigated with these two test ionograms. The maximum error resulting from the use of an inverse cube field model was 10.4 km for the high altitude profiles and 0.22 km for the low altitude profile. It was also found that no significant error is introduced if the magnetic variation is assumed to follow the inverse cube law within each lamination.

6. Additional Considerations

The preceding error study was limited to an investigation of errors arising from the numerical inversion of the group height integral. Systematic errors usually less than 30 km can also be present in the original p'-f data (see Franklin et al in this issue and "Comparisons between Topside and Ground-Based Soundings", Jackson, in this issue). The validity of the assumption of vertical propagation was not discussed in the present paper. It is shown in a separate paper ("Comparisons between Topside and Ground-Based Soundings", Jackson, in this issue) that the assumption of vertical propagation is a fairly good approximation in many cases, particularly for low altitude ionograms.

Small errors (usually less than 5 kilometers) can also arise if allowance is not made for the fact that the sounder altitude can change by a few kilometers during a sounding.

VI. CONCLUSION

The techniques presently available for the analysis of topside ionograms can yield electron density profiles with an altitude accuracy of the order of a few kilometers, provided the p'-f data is free of scaling and of systematic errors, and provided the soundings correspond to vertical propagation. In actual practice errors in N(h) analysis are due primarily to the accuracy of the p'-f data and to deviations from vertical propagation.

FORMULAS FOR GROUP AND REFRACTIVE INDICES

1. Basic Formulas

The group refractive index n' for a radio wave of frequency f is defined as the free space velocity of light divided by the group velocity of the wave. The fundamental formula for n' is:

$$n' = n + f \frac{\partial n}{\partial f} \tag{A-1}$$

where n is the real part of the refractive index of the medium. The index n is given by the well known Appleton Hartree formula, namely:

$$n = \sqrt{1 - \frac{X}{1 - \frac{Y_T^2}{2(1-X)} \pm \sqrt{\left[\frac{Y_T^2}{2(1-X)}\right]^2 + Y_L^2}}} \tag{A-2}$$

where

$X = N/(12{,}400f^2) = \frac{(fN)^2}{f^2}$

N = electrons/cc

fN = electron plasma frequency

f = frequency (MHz)

Y = fH/f

fH = 2.8B MHz

B = (terrestrial) magnetic induction in gausses

$Y_T = Y \sin \phi$

$Y_L = Y \cos \phi$

ϕ = angle between propagation vector and magnetic field

$\pm$ = positive sign in front of square root is for ordinary ray; negative sign is for extraordinary ray.

For the vertical propagation assumed in the analysis:

$$Y_T = Y \text{ Cos } \theta$$

$$Y_L = Y \text{ Sin } \theta$$

where

θ = angle of magnetic dip

The reflection conditions are X=1 for the ordinary ray (except when θ is exactly 90^o) and X=1-Y for the extraordinary ray.

The evaluation of $\frac{\partial n}{\partial f}$ is fairly complicated since n is a function of X and Y and both of these parameters are functions of f. The calculations are simplified considerably, however, when θ is either 0 or 90 degrees, i.e., when the earth's magnetic field is either perpendicular to (transverse propagation) or parallel to (longitudinal propagation) the direction of the wave propagation. For these two limiting cases it is also possible to evaluate analytically the group height integral $\int n\, dh$ and hence check the accuracy of the numerical integration technique which is needed for the general case (i.e., θ neither 0, nor 90 degrees).

2. Special Cases

a. Transverse Propagation (θ=0; Y_T=Y; Y_L=0)

In this case formulas (A-2) and (A-1) give:

for the ordinary ray:

$$n = \sqrt{1-X} \qquad \text{(A-3)}$$

$$n' = 1/n \qquad \text{(A-4)}$$

for the extraordinary ray:

$$n = \sqrt{1 - \frac{X(1-X)}{1-X-Y^2}} \qquad \text{(A-5)}$$

$$n' = \frac{1}{n}\left[1 + \frac{XY^2}{(1-X-Y^2)^2}\right] \qquad \text{(A-6)}$$

b. Longitudinal Propagation ($\theta=90^o$, $Y_L=Y$, $Y_T=0$)

In this case formulas (A-2) and (A-3) give:

for the ordinary ray:

$$n = \sqrt{1 - X/(1+Y)} \qquad \text{(A-7)}$$

$$n' = \frac{1}{n}\left[1 - \frac{XY}{2(1+Y)^2}\right] \qquad \text{(A-8)}$$

for the extraordinary ray:

$$n = \sqrt{1 - X/(1-Y)} \qquad \text{(A-9)}$$

$$n' = \frac{1}{n}\left[1 + \frac{XY}{2(1-Y)^2}\right] \qquad \text{(A-10)}$$

3. Doupnik's Formulas for the Group Index.

The group index can be evaluated by substituting into Eq. (A-1) the value of n given by Eq. (A-2). The resulting formula for the group index is complicated and it does not lend itself to accurate numerical calculations. An expression for n', which is compact and also well suited for numerical analysis, can be obtained by making a substitution suggested by J. R. Doupnik (private communication), namely:

$$\tan \alpha = \frac{Y_T^2}{2Y_L(1-X)} \qquad (A\text{-}11)$$

and evaluating equation A-1 yields:

$$n' = \frac{1}{n}\left[1 + \frac{X(1-S)}{2S^2}\left(1 + e\,\frac{1+X}{1-X}\,\mathrm{Sin}\,\alpha\right)\right] \qquad (A\text{-}12)$$

where:

$$n = \sqrt{1 - \frac{X}{S}} \qquad (A\text{-}13)$$

$S = 1 + Y_L \frac{\mathrm{Cos}\alpha}{1+\mathrm{Sin}\alpha}$ for the ordinary ray

$e = -1$ for the ordinary ray

$S = 1 - Y_L \frac{1+\mathrm{Sin}\alpha}{\mathrm{Cos}\alpha}$ for the extraordinary ray

$e = +1$ for the extraordinary ray

The above formulas are not valid for $Y_L = 0$. In this case formulas (A-3), (A-4), (A-5) and (A-6) are used in lieu of (A-11), (A-12) and (A-13).

APPENDIX B

ACCURACY OF GROUP HEIGHT INTEGRAL CALCULATIONS

The evaluation of $\int_{h_1}^{h_2} n'dh$ requires both accurate values of the group index and an accurate integration technique. The accuracy of the n' calculations can be checked against Becker's tables (1960). The integration technique is critical only for the last lamination, i.e., for the lamination which includes the reflection point (where n' becomes infinite). Hence the method of integration must be checked with an integral of the form:

$$I = \int_{h_{R-\Delta h}}^{h_R} n'dh \qquad \text{(B-1)}$$

where the upper limit of integration h_R is the reflection point. The accuracy of the numerical integration technique can be investigated in two different ways. One way is to perform the numerical integration several times, each time increasing the number of sampling points L. If the results become constant for L>K, then K sampling points yield an accurate answer. Another method is to examine one of the special cases when the integration can be performed analytically. The test discussed here was done using the n' function for the extraordinary ray, longitudinal propagation and constant Y. This yields an integral which can be evaluated analytically. A linear in log N lamination was used (see Eq. 19) giving:

$$h = h_{j-1} + a_j (\ln N - \ln N_{j-1})$$

and

$$dh = a_j \frac{dN}{N} = a_j \frac{dX}{X}$$

Changing to the variable X in Eq. (B-1) gives:

$$I = a_j \int_{1-Y-\epsilon}^{1-Y} \frac{n'}{X} dX \qquad (B-2)$$

Since a_j is outside of the integral, it can be assumed to be unity for the purpose of checking the integration technique. In this case n' is given by Equation (A-10), which can be written

$$n' = \frac{1+bX}{\sqrt{1+aX}} \qquad (B-3)$$

where $a = \frac{-1}{1-Y}$ and $b = \frac{Y}{2(1-Y)^2}$

For any specified value of Y, the quantities a and b are constants. Substituting n' from Eq. (B-3) into Eq. (B-2) yields:

$$I = \int_{1-Y-\epsilon}^{1-Y} \left[\frac{1+bX}{X\sqrt{1+aX}} \right] dX \qquad (B-4)$$

The recommended substitution for the numerical evaluation of Eq. (B-4) is to let:

$$t^2 = 1-X/(1-Y)$$

giving: $$2tdt = - dX/(1-Y)$$

The integration limits are:

$$t_1 = (1 - \frac{1-Y-\epsilon}{1-Y})^{\frac{1}{2}} = \sqrt{\frac{\epsilon}{1-Y}}$$

and $$t_2 = 0$$

After making the above change in variable, and noting that for this special longitudinal case $t = \sqrt{1+aX}$, Eq. (B-4) becomes:

$$I = \int_0^{\sqrt{\frac{\varepsilon}{1-Y}}} 2(1-Y)\left(\frac{1+bX}{X}\right) dt \qquad \text{(B-5)}$$

where: $X = (1-t^2)(1-Y)$.

The analytical solution of Eq. (B-4) is:

$$I = \left[\frac{2b\sqrt{1+aX}}{a} - \ln \left(\frac{1+\sqrt{1+aX}}{1-\sqrt{1+aX}}\right) \right]_{X=1-Y-\varepsilon}^{X=1-Y}$$

In the above expression, the ratio of the integration limits $(1-Y)/(1-Y-\varepsilon)$ is the ratio of the values of X at the two boundaries. Since X is proportional to N, this ratio is also the electron density ratio N_2/N_1, where N_1 is the initial (or minimum) density and N_2 is the last (or maximum) density for the lamination. The numerical and analytical integrations were carried out for values of Y ranging from 0.1 to 0.9 (for routine analysis Y will seldom exceed a value of 0.90) and for electron density ratios $(1-Y)/(1-Y-\varepsilon)$ ranging from 1.01 to 2.0. The numerical integration was performed with the indicated change of variable using a 3 point Gaussian technique, and also without making a change of variable with a 7 point and a 16 point Gaussian technique.

The errors arising from the various numerical integration techniques are shown in table B-1. The error is roughly constant and quite substantial for each Gaussian integration where no change in variable was made (4.7 to 5.8 percent with the 7 point Gaussian and 2.1 to 2.6 percent with the 16 point Gaussian). When the change in variable is made, the error is less than 0.1 percent for all conditions considered and only 3 points are required in the Gaussian integration. This remarkable improvement in accuracy is obtained because the integrand in Eq. (B-5) is a very slowly changing function. For the special case investigated here ($\theta=0$) the curves representing the integrand as a function of t are parallel to each other as the parameter Y is changed. This is

readily seen for the case $\theta=0$; since then:

$$2(1-Y)n't/X = \frac{2}{1-t^2} + \frac{Y}{1-Y}$$

The integrand obtained for the general case ($\theta\neq0$) has a similar slow variation as a function of t as can be seen from Fig. B-1, and consequently the data shown in table B-1 is also indicative of the improvement in accuracy which can be obtained for arbitrary values of θ when a change in variable is made.

In order to apply these results to the actual N-h analysis, it is necessary to calculate the density ratios which are obtained with the GSFC criterion for the selection of data points. The density ratios depend upon fH and fx at the satellite and also upon the frequency increments specified by the criterion. Typical ratios are shown in Fig. B-2. It is seen that the ratios are always less than 1.6. Hence the maximum error obtained using the 3 point Gaussian with change of variable is less than 0.020. Thus for the extraordinary ray this method is at least two (and typically three to four) orders of magnitude more accurate than the 16 point Gaussian with no change in variable.

Y	Density Ratio in Lamination				
	1.01	1.10	1.40	1.60	2.00
7 POINT GAUSSIAN - NO CHANGE IN VARIABLE					
.1	5.79	5.63	5.23	5.02	4.70
.3	5.79	5.66	5.29	5.11	4.82
.5	5.79	5.68	5.39	5.23	4.98
.7	5.79	5.72	5.51	5.39	5.21
.9	5.80	5.77	5.69	5.64	5.56
16 POINT GAUSSIAN - NO CHANGE IN VARIABLE					
.1	2.63	2.56	2.38	2.28	2.14
.3	2.63	2.57	2.41	2.32	2.19
.5	2.63	2.58	2.45	2.38	2.27
.7	2.63	2.60	2.50	2.45	2.37
.9	2.64	2.62	2.50	2.56	2.53
3 POINT GAUSSIAN - CHANGE IN VARIABLE					
.1	0.000025	0.000044	0.0041	0.014	0.065
.3	0.000025	0.000038	0.0036	0.013	0.058
.5	0.000025	0.000031	0.0029	0.011	0.048
.7	0.000025	0.000021	0.0021	0.008	0.035
.9	0.000025	0.000007	0.0008	0.003	0.015

Table B-1. Percent error in the evaluation of the group height integral $\int_{1-Y-\epsilon}^{1-Y} \frac{n'}{x}\, dx$ as a function of Y and of the electron density ratio $(1-Y)/(1-Y-\epsilon)$ for various integration techniques. Calculations were performed for the case of longitudinal propagation.

APPENDIX C

N(h) CALCULATIONS USING THE EXTRAORDINARY TRACE AND PARABOLIC-IN LOG (N) LAMINATIONS.

1. General Procedure

It was indicated earlier (Section II of the text) that most of the topside N(h) profiles have been derived from the analysis of the extraordinary ray echoes. The principles of the analysis technique (lamination method) were introduced in Section III and discussed further in Section IV. In Section V it was shown that very accurate results can be obtained if the laminations are assumed to be parabolic-in-log (N) with continuous slopes at the lamination boundaries (see Fig. 4). The present appendix is devoted to a detailed description of the (X) data analysis using parabolic-in-log (N) laminations and assuming vertical propagation. The notation used is the same as in Section III, and for convenience a few formulas previously given are repeated here.

The $j^{\underline{th}}$ lamination is defined by:

$$h = h_{j-1} + a_j \ln \frac{N}{N_{j-1}} + b_j (\ln \frac{N}{N_{j-1}})^2 \qquad \text{(C-1)}$$

where

$$a_j = a_{j-1} + 2b_{j-1} \ln \frac{N_{j-1}}{N_{j-2}} \qquad \text{(C-2)}$$

The above formulas apply to all laminations except the first one, which is assumed to be linear-in-log (N), i.e., $b_1 = 0$. The calculations also require that all expressions in (C-1) and (C-2) be finite. This requirement will be met only if the N(h) function is monotonic.

In the N(h) calculations, the laminations are determined one at a time, in the order (h_0, h_1), (h_1, h_2), (h_2, h_3) etc. Hence all laminations between the altitudes h_0 and h_{j-1} are known, when the calculation of the $j^{\underline{th}}$ lamination is performed. Let f_j represent the frequency of the extraordinary wave reflected from the unknown height h_j. The virtual height h'_j is given by:

$$p'_j = \int_{h_1}^{h_0} n'dh + \int_{h_2}^{h_1} n'dh + \ldots + \int_{h_j}^{h_{j-1}} n'dh \qquad \text{(C-3)}$$

$$= DP + \int_{h_j}^{h_{j-1}} n' dh \qquad (C-4)$$

where DP represents the delay in the previous laminations. The calculation of DP presents no special problem, since it involves calculation of integrals in which all parameters are known. The process for calculating DP will be illustrated later. For the present discussion (calculation of j^{th} lamination) it will be assumed that DP is known.

2. Initial Calculation of j^{th} lamination (Constant Y)

The reflection conditions at the bottom of the j^{th} lamination can be written in terms of the X and Y notation of Appendix A as follows:

$$X_j = 1 - Y_j \qquad (C-5)$$

where

$$Y_j = \frac{(fH)_j}{f_j} \qquad (C-6)$$

Equation C-1 can be expressed in terms of X by noting that

$$\frac{N}{N_{j-1}} = \frac{X}{X_{j-1}} \qquad (C-7)$$

Making the substituting indicated by Eq. (C-7) in Eq. (C-1) and differentiating Eq. (C-1) yields:

$$dh = \left[a_j + 2b_j \ln\left(\frac{X}{X_{j-1}}\right)\right] \frac{dX}{X} \qquad (C-8)$$

Substituting the above value of dh in Eq. (C-4) yields:

$$p'_j = DP + a_j \int_{X_j}^{X_{j-1}} \frac{n}{X}\, dX + 2b_j \int_{X_j}^{X_{j-1}} \frac{n}{X} \ln\left(\frac{X}{X_{j-1}}\right) dX \qquad (C-9)$$

Letting $t^2 = 1-X/(1-Y_j)$ and noting that $dX = -2(1-Y_j)t\ dt$ gives

$$p'_j = DP - a_j \int_o^{t_{j-1}} 2(1-Y_j)\ \frac{n'}{X}\ t\ dt$$

$$- b_j \int_o^{t_{j-1}} 4(1-Y_j)\ \frac{n'}{X}\ \ln\left(\frac{X}{X_{j-1}}\right)\ t\ dt \qquad (C\text{-}10)$$

To simplify the notation of Eq. C-10, the parameter X was retained in the formula. In Eq. C-10, however, X is the following function of t:

$$X = (1-t^2)(1-Y_j) \qquad (C\text{-}11)$$

Similarly, since n' is a function of X, Y and θ, the values of X entering into the calculation of n' are those given by Eq. C-11. Since the value of Y_j is not known initially, it is necessary to use an estimated value of Y, to compute the integrals in Eq. (C-10). One method is to let $Y_j = Y_{j-1}$ and to assume that Y is constant within the lamination and equal to Y_{j-1}. All the parameters are then known in Eq. (C-10) and the integrals can be evaluated. Representing the integrals associated with a_j and b_j by S_A and S_B respectively, yields:

$$b_j = (DP - p'_j - a_j S_A)/S_B \qquad (C\text{-}12)$$

The above initial estimate of Y_j can cause the iteration process to fail. For this reason a different procedure is used as indicated in section 4 of Appendix C.

3. Iteration With Variable Y

The approximate answer thus obtained for the lamination can be refined by an iteration process, in which Y_j is computed for the calculated value of h_j and in which the values of Y entering into the n' calculations are computed by assuming that Y decreases from the value Y_{j-1} at the top of the lamination to the value Y_j at the bottom of the lamination according to:

$$Y = \frac{K}{(R + h)^3} \qquad (C\text{-}13)$$

The constant K and the earth's radius R in Eq. (C-13) can be eliminated by making use of the boundary conditions:

$$Y_j(R + h_j)^3 = Y_{j-1}\,(R + h_{j-1})^3 = K \qquad (C\text{-}14)$$

To express Y in terms of Y_j, Y_{j-1} and h, Eqs. (C-13) and (C-14) are written:

$$R + h = K/Y^{1/3} \qquad (C\text{-}15)$$

$$R + h_j = K/Y_j^{1/3} \qquad (C\text{-}16)$$

$$R + h_{j-1} = K/Y_{j-1}^{1/3} \qquad (C\text{-}17)$$

from which

$$h - j = K(Y^{-1/3} - Y_j^{-1/3}) \qquad (C\text{-}18)$$

$$h_{j-1} - h_j = K(Y_{j-1}^{1/3} - Y_j^{-1/3}) \qquad (C\text{-}19)$$

The constant K is eliminated by dividing Eq. (C-18) by Eq. (C-19). Solving the resulting equation for Y yields:

$$Y = \frac{Y_j}{\left\{1 + \left[\left(\frac{Y_j}{Y_{j-1}}\right)^{1/3} - 1\right]\frac{(h-h_j)}{(h_{j-1}-h_j)}\right\}^3} \qquad (C\text{-}20)$$

The values of h to be used in Eq. (C-20) should be those corresponding to the values of X. It is therefore important to note that the b_j obtained from Eq. (C-12) was based upon the assumption:

$$X_j = 1 - Y_{j-1} \qquad (C\text{-}21)$$

Hence to be consistent the altitude h_j must be calculated according to the formula:

$$h_j = h_{j-1} + a_j \ln\left(\frac{X_j}{X_{j-1}}\right) + b_j \left[\ln\left(\frac{X_j}{X_{j-1}}\right)\right]^2 \qquad (C-22)$$

where $X_j = 1-Y_{j-1}$

If Y_j is now redefined in terms of h_j, (giving $X_j = 1-Y_j$) Eq. (C-22) will no longer yield the same value of h_j at the reflection point. In order to proceed with the iteration (and in particular make sure that Eq. (C-20) will keep Y between Y_{j-1} and Y_j), we must either redefine h_j in terms of $X_j = 1-Y_j$, or recompute b_j so that Eq. (C-22) gives the same value of h_j for the new X_j. In the GSFC program, the computed value of h_j is preserved. The parameters Y_j, X_j, and b_j are redefined prior to the iteration process. Iteration is continued until the successive values obtained for h_j agree to within 0.01 km. When this happens the difference between the b_j computed from Eq. (C-12) and the b_j reevaluated prior to iteration becomes insignificant. When the desired convergence is achieved, the final value of b_j is the value computed from Eq. (C-12) and the final value of h_j correspond to the Y_j and X_j obtained from the previous calculation. Hence the final compromise is made on fH_j which is actually computed (and stored in the program) for an altitude slightly different than h_j (the altitude difference, however, being less than 10 meters).

Returning to the postponed discussion of DP of Eq. (C-4), it is seen that DP involves a summation of integrals identical to those of the $j^{\underline{th}}$ lamination, except that the limits are different, but known when the $j^{\underline{th}}$ lamination is calculated. These integrals are also evaluated making use of the change of variable $t^2 = 1 - X/(1-Y_j)$, and using Eq. (C-20) to vary Y within the lamination.

For the first lamination, which is assumed linear-in-log N, the coefficient b is zero and Eq. (C-10) is solved for the coefficient a. Actually the first calculation made on the $j^{\underline{th}}$ lamination is also based upon a linear-in-log N method; this

yields a good estimate of the value of h_j, which is then used as the starting point for the iteration using the parabolic-in-log N technique.

4. Convergence of the iteration process. (Initial value of Yj)

The p'-f to N(h) conversion discussed in this paper requires that the p'-f trace be well defined and equivalent to a continuous curve. This requirement is easily met on topside ionograms, because in the topside ionosphere N usually decreases monotonically with h. Such an N(h) distribution is implicitly assumed in the parabolic-in-log N lamination technique and also in the transformation $t^2 = 1-X/(1-Y_j)$.

The existence of a continuous trace on a topside ionogram usually implies that N decreases monotonically with h. Exceptions to this general rule are theoretically possible for the X trace. The reflection condition:

$$fx = \frac{fH}{2} + \tfrac{1}{2}\sqrt{4(fN)^2 + (fN)^2}$$

shows that echoes can be continuously received as a function of fx, provided the quantity $\left[4(fN)^2 + fH^2\right]$ increases monotonically with distance below the sounder. Since fH increases as a function of depth below the sounder, this increase could overcompensate a decrease in N (Lockwood, private communication). In the present N(h) reduction technique, such a situation is readily detected and it results in a rejection of the ionogram.

Even if the profile decreases monotonically with altitude, the iteration process (based upon the initial assumption $Y_j = Y_{j-1}$) may not converge if the profile is sufficiently steep. The permissible values of gyrofrequencies at the bottom of the lamination range from the value at the top of the lamination fH_{j-1} to a maximum value fH_{jM} corresponding to the minimum permissible increase in density. Thus, if we define the minimum permissible increase in density as 0.1 percent, the quantity fH_{jM} is defined by:

$$fx_j\,(fx_j - fH_{jM}) = (1.001)\,fx_{j-1}(fx_{j-1} - fH_{j-1}) \qquad \text{(C-23)}$$

True height calculations yield different answers for h_j as fH_j is varied from fH_{j-1} to fH_{jM}. The basic purpose of the iteration process is to find from all the permissible values of h_j, the particular height h_j at which the fH_j used in the true height calculation is the same as the actual value of fH_j at the altitude h_j. The above iteration process is illustrated by Fig. C-1, which shows how true-height calculations are influenced by the assumed value of fH at the bottom of a lamination. The curves L_1, L_2 and L_3 show the heights h_1 at the bottom of the first lamination as a function of fH_1 over the permissible range of fH_1 for various assumed values of p'_1 on the extraordinary trace. The assumed conditions at the top of the lamination (i.e., at the satellite altitude) were hS= 2000 km, fHs = 0.45 MHz and fxS = 0.50. At the bottom of the lamination, it was assumed that f_1 = 0.52 MHz. An inverse-cube variation was assumed for fH. For p'_1 = 1800 km, the resulting heights are given by the curve L_1. Curve M shows the actual gyrofrequency at the altitudes shown. The correct height is therefore given by the intersection of curves L_1 and M. If the initial assumption is fH_1 = fHS, the first value of h_1 would correspond to A_1. The iteration would then be performed using fH at B_1, which is the correct fH at the altitude of A_1. This would yield a new value of h_1, namely that corresponding to C_1. The second iteration is performed using the fH value at D_1. It is seen graphically that the process converges to the point O_1. The same process, however, will not converge on curve L_2, although there is a solution at O_2. If the calculation is started with the maximum permissible value of fH, the initial height will be at P_1 on curve L_1 and at P_2 on curve L_2. It is seen that the process will then always converge, if there is a solution. Curve L_3 is an example in which there is no solution such that the density at the bottom of the first lamination is greater than the density at the satellite.

In view of the above consideration, the GSFC program performs the initial calculation of the laminations using the value of fH_j defined by Eq. (C-23), provided fH_{jM} is less than 1.15 fH_{j-1}. This upper limit was set for fH_{jM} because at lower altitudes where the density increases rapidly with depth, Eq. (C-23) leads to unreasonably high values of fH_{jM}.

REFERENCES

Bauer, S. J.,"On the Structure of the topside ionosphere",Journal of the Atmospheric Sciences, Vol. 19, No. 3, pp. 276-278, May, 1962.

Bauer, S. J., Blumle, L. J., Donley, J. L., Fitzenreiter, R. J. and Jackson, J. E., "Simultaneous Rocket and Satellite Measurements of the Topside Ionosphere", J. Geophys. Res., 69, pp. 186-189, Jan. 1, 1964.

Becker, W., "Tables of Ordinary and Extraordinary Refractive Indices, group refractive indices and $h'_{o,x}(f)$ - curves for standard ionospheric layer models," Mitteilungen aus dem Max-Plank-Institut fur Aeronomie, 1960.

Budden, K. G., "Radio Waves in the Ionosphere," University Press, Cambridge, England, 1961.

Calvert, W., "Oblique Z-mode echoes in the Topside Ionosphere," Journal of Geophys. Res., Vol. 71, No. 23, pp. 5579-5583, Dec. 1, 1966.

Doupnik, J. R. and Schmerling, E. R., "The reduction of ionograms from the bottomside and topside," Journal of Atmospheric and Terrestrial Physics, Vol. 27, pp. 917 to 941, Sept. 1965.

Fitzenreiter, R. J. and Blumle, L. J., "Analysis of Topside Sounder Records," Journal of Geophys. Res., Vol. 69, No. 3, pp. 407-415, Feb. 1, 1964.

Jackson, J. E., "A New Method for Obtaining Electron Density Profiles from P'-f Records," Journal of Geophys. Res., Vol. 61, pp. 107-127, March 1956.

Jackson, J. E., "The Analysis of Topside Ionograms," GSFC Report X-615-67-452, Sept. 1967.

Kelso, John M., "Radio Ray Propagation in the Ionosphere," McGraw-Hill, Inc., 1964.

Paul, A. K. and Wright, J. W., "Some Results of a New Method for Obtaining Ionospheric N(h) profiles and their bearing on the Structure of the lower F region," Journal of Geophys. Res., Vol. 68, No. 19, pp. 5413-5420, October 1, 1963.

Poeverlein, H., Z. Angew. Phys. 1951, 3, 135.

Ratcliffe, J. A., "The Magneto-ionic Theory," University Press. Cambridge, England, 1962.

Shinn, D. H. and Whale, H. A., "Group Velocities and Group Heights from the Magneto-ionic Theory," Journal of Atmospheric and Terrestrial Physics. Vol. 2, pp. 85-105, 1952.

FIGURE CAPTIONS

Fig. 1. Typical Group Velocity Curves.

Fig. 2. Example of an Alouette II ionogram with excellent Z, O and X traces.

Fig. 3 Electron densities obtained from the ionogram of Fig. 3, doing independent N(h) analysis on each of the Z, O and X traces. The points shown in the graph were selected from the computed points. For the sake of clarity, overlapping points were omitted, except at the ends of the profile.

Fig. 4. Lamination Model.

Fig. 5. Ionospheric profiles used for error studies.

Fig. 6. Ionogram corresponding to the high density profile of Fig. 5. Points shown are those obtained using the author's scaling criterion.

Fig. 7. Ionogram corresponding to the low density profile of Fig. 5. Points shown are those obtained using the author's scaling criterion.

Fig. 8. Relative accuracy of parabolic-in-log N and linear-in-log N techniques for the 24-point analysis.

Fig. 9. Relative accuracy of parabolic-in-log N and linear-in-log N techniques for the 13-point analysis.

Fig. 10. Errors introduced when iteration is not used. Graphs shown are for the linear-in-log N and for the parabolic-in-log N methods. Point A is common to both graphs and computed using the linear-in-log N method. The error on the next point is much smaller using the linear (B_1) than using the parabolic-in-log N method (B_2).

Fig. 11. Errors introduced when the group height integrals are evaluated without making the change of variable $t^2 = 1 - X/(1-Y_R)$.

Fig. 12. Errors introduced in ionogram analysis when either the integrand is infinite at the reflection point, or when iteration is not performed. The calculations were based upon laminations parabolic-in-log N. Hs is the satellite altitude.

Fig. B-1. Behavior of integrand in extraordinary ray group height integrals as a result of the change of variable $t^2 = 1-X/(1-Y)$.

Fig. B-2. Size of laminations (in terms of density ratios) resulting from the author's scaling criterion for various values of gyrofrequencies and densities at the satellite. The gyrofrequency was assumed to be independent of altitude, which yields an overestimate of the ratios.

Fig. C-1. Computed altitude for the bottom of a lamination as a function of gyrofrequency. The minimum gyrofrequency is the value at the satellite, and the maximum gyrofrequency is based upon an essentially constant density within the lamination. The actual gyrofrequency as a function of altitude is also indicated. The correct value of gyrofrequency at the bottom of the lamination is the intersection of the two curves. The purpose of the iteration process is to find this intersection point.

Fig. 1

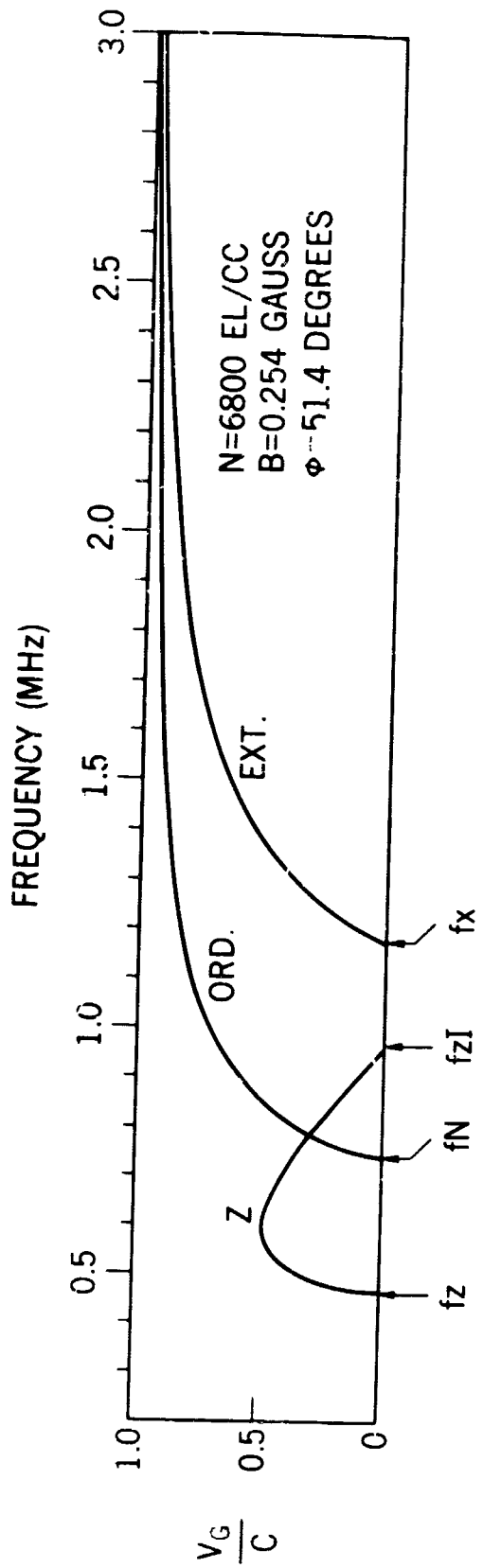
FREQUENCY (MHz)
3.0
2.5
2.0
1.5
1.0
0.5
N=6800 EL/CC
B=0.254 GAUSS
Φ=51.4 DEGREES
EXT.
ORD.
Z
fx
fzI
fN
fz
1.0
0.5
0
$\frac{V_G}{C}$

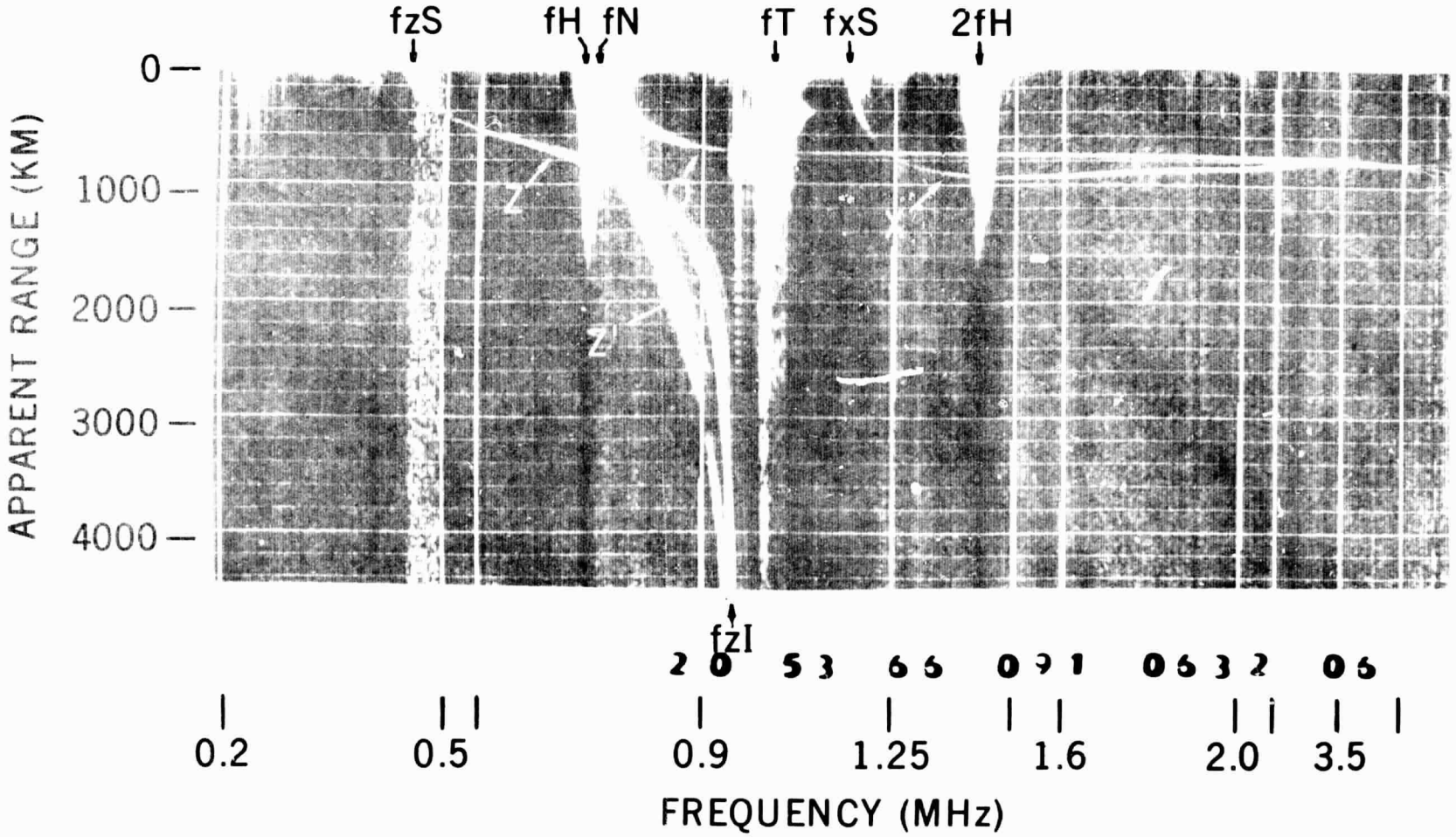
fzS
fH
fN
fT
fxS
2fH
0
1000
2000
3000
4000
APPARENT RANGE (KM)
fzI
0.2
0.5
0.9
1.25
1.6
2.0
3.5
FREQUENCY (MHz)

Fig. 2

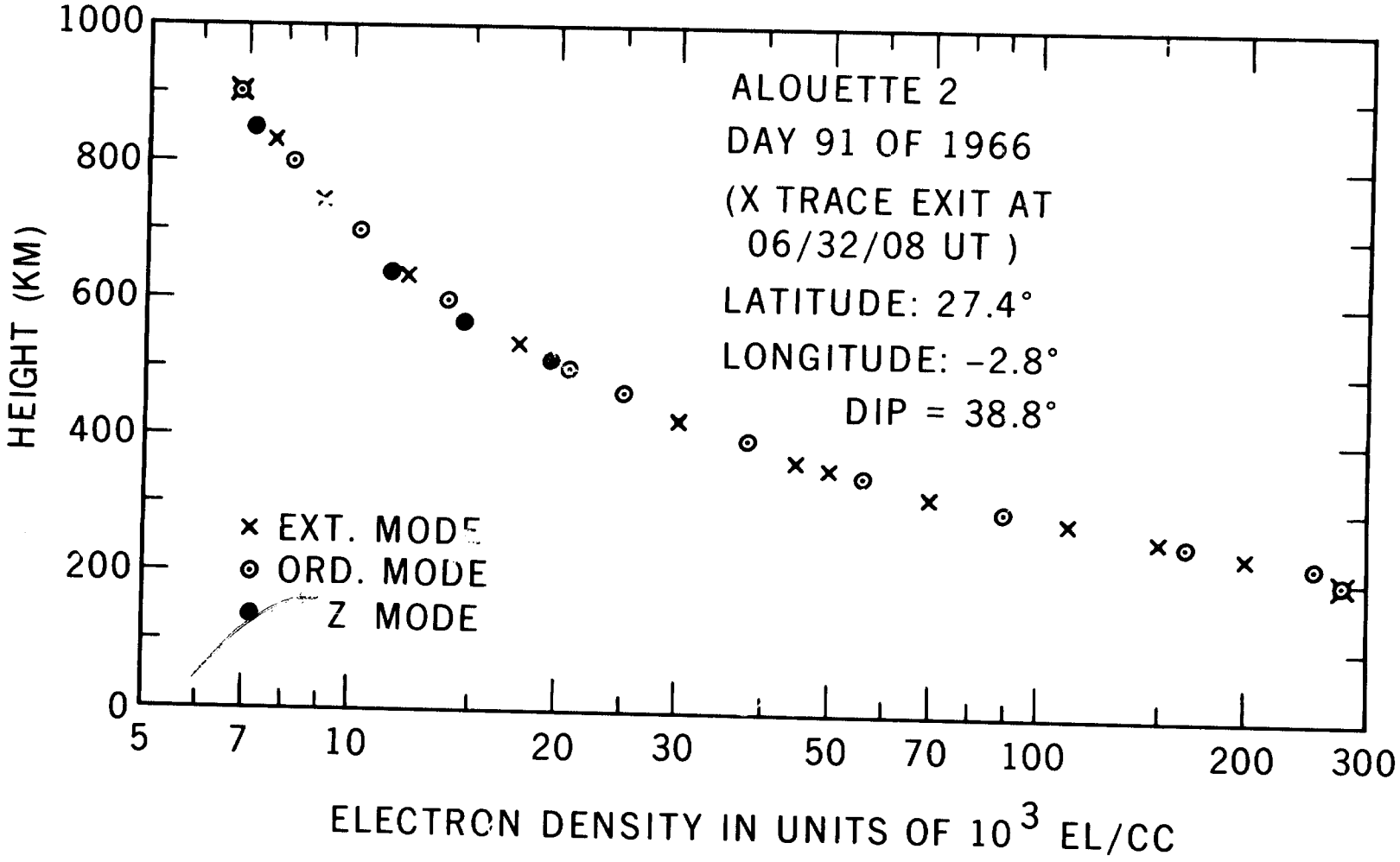
ALOUETTE 2
DAY 91 OF 1966
(X TRACE EXIT AT
06/32/08 UT)
LATITUDE: 27.4°
LONGITUDE: -2.8°
DIP = 38.8°
× EXT. MODE
⊙ ORD. MODE
● Z MODE
HEIGHT (KM)
1000
800
600
400
200
0
5
7
10
20
30
50
70
100
200
300
ELECTRON DENSITY IN UNITS OF 10^3 EL/CC

Fig. 3

Fig. 4

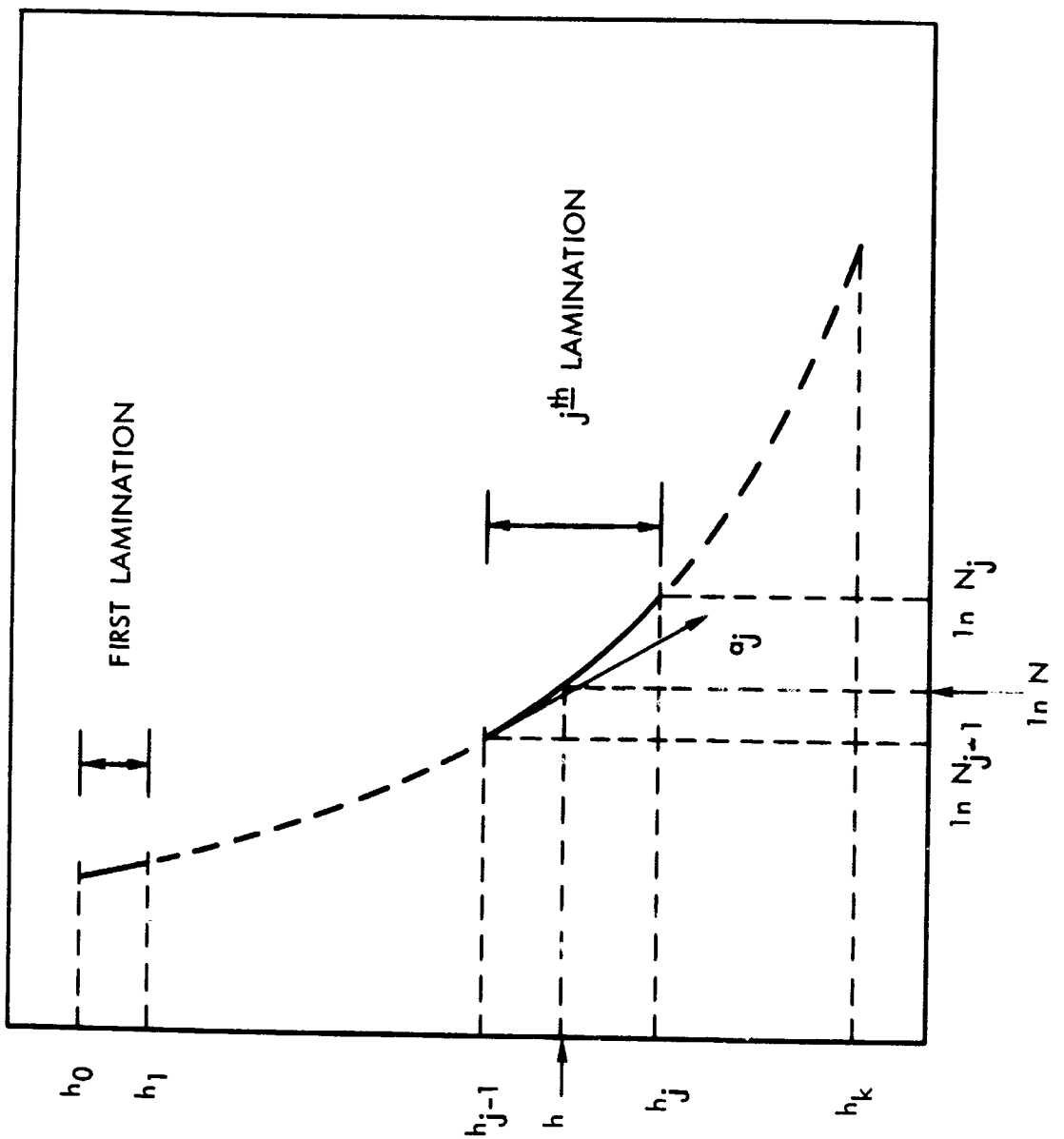
FIRST LAMINATION
j^th LAMINATION
a_j
ln N_j
ln N
ln N_j-1
h_0
h_1
h_j-1
h
h_j
h_k

Fig. 5

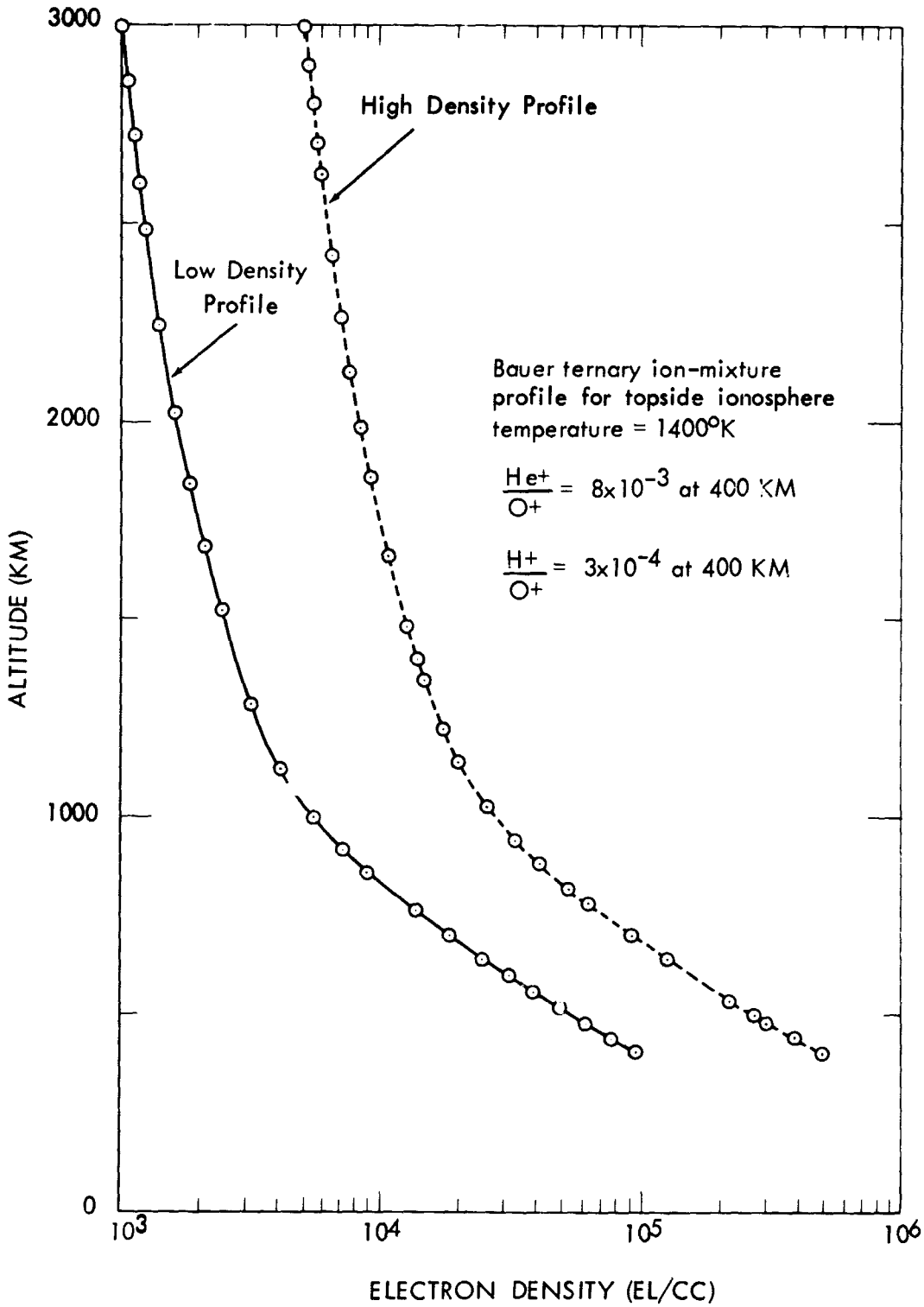
3000
2000
1000
0
ALTITUDE (KM)
High Density Profile
Low Density Profile
Bauer ternary ion-mixture profile for topside ionosphere temperature = 1400°K
He+/O+ = 8x10^-3 at 400 KM
H+/O+ = 3x10^-4 at 400 KM
10^3
10^4
10^5
10^6
ELECTRON DENSITY (EL/CC)

Fig. 6

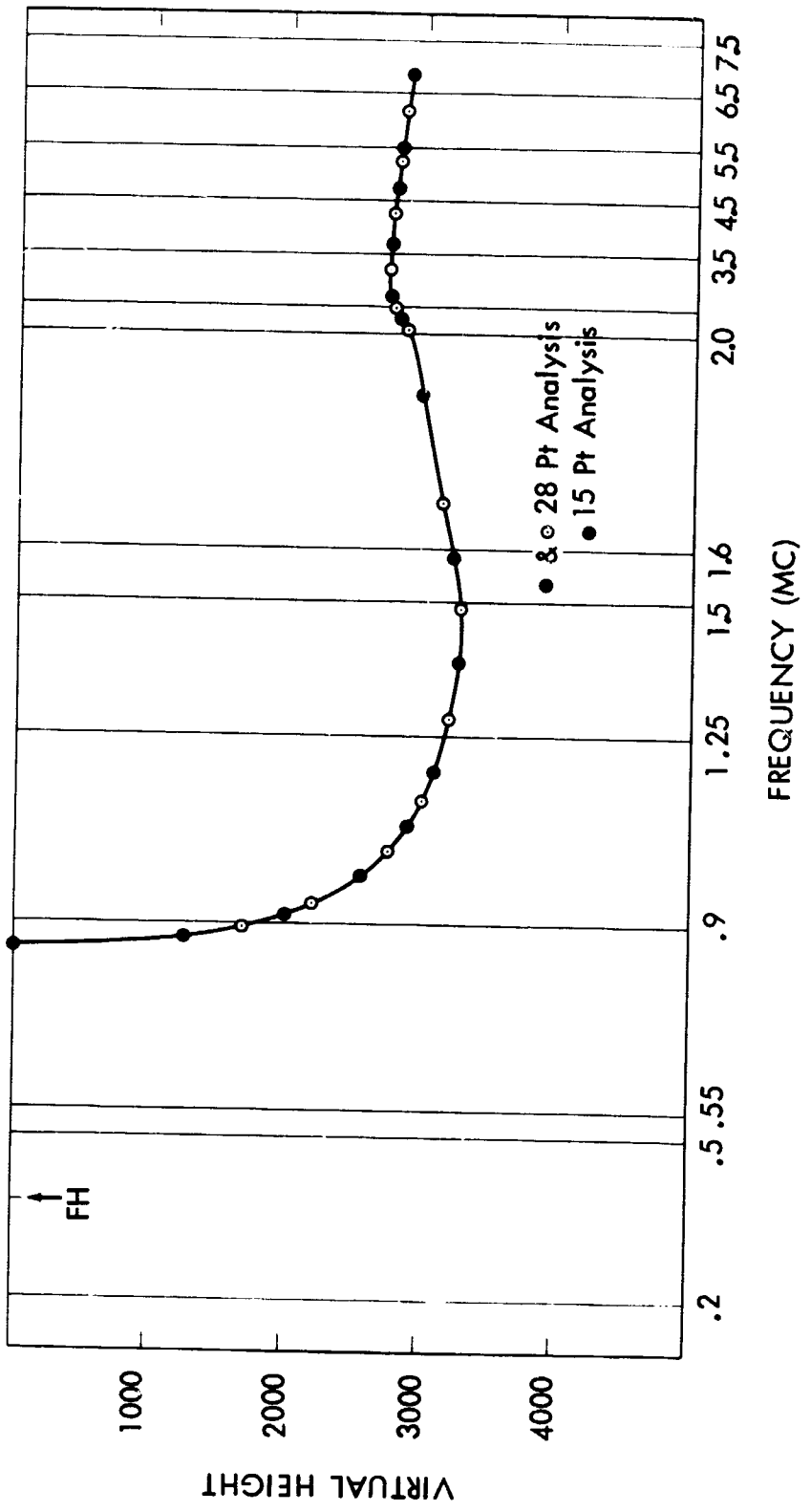
VIRTUAL HEIGHT
1000
2000
3000
4000
FH
.2
.5
.55
.9
1.25
1.5
1.6
2.0
3.5
4.5
5.5
6.5
7.5
FREQUENCY (MC)
● & ○ 28 Pt Analysis
● 15 Pt Analysis

Fig. 7

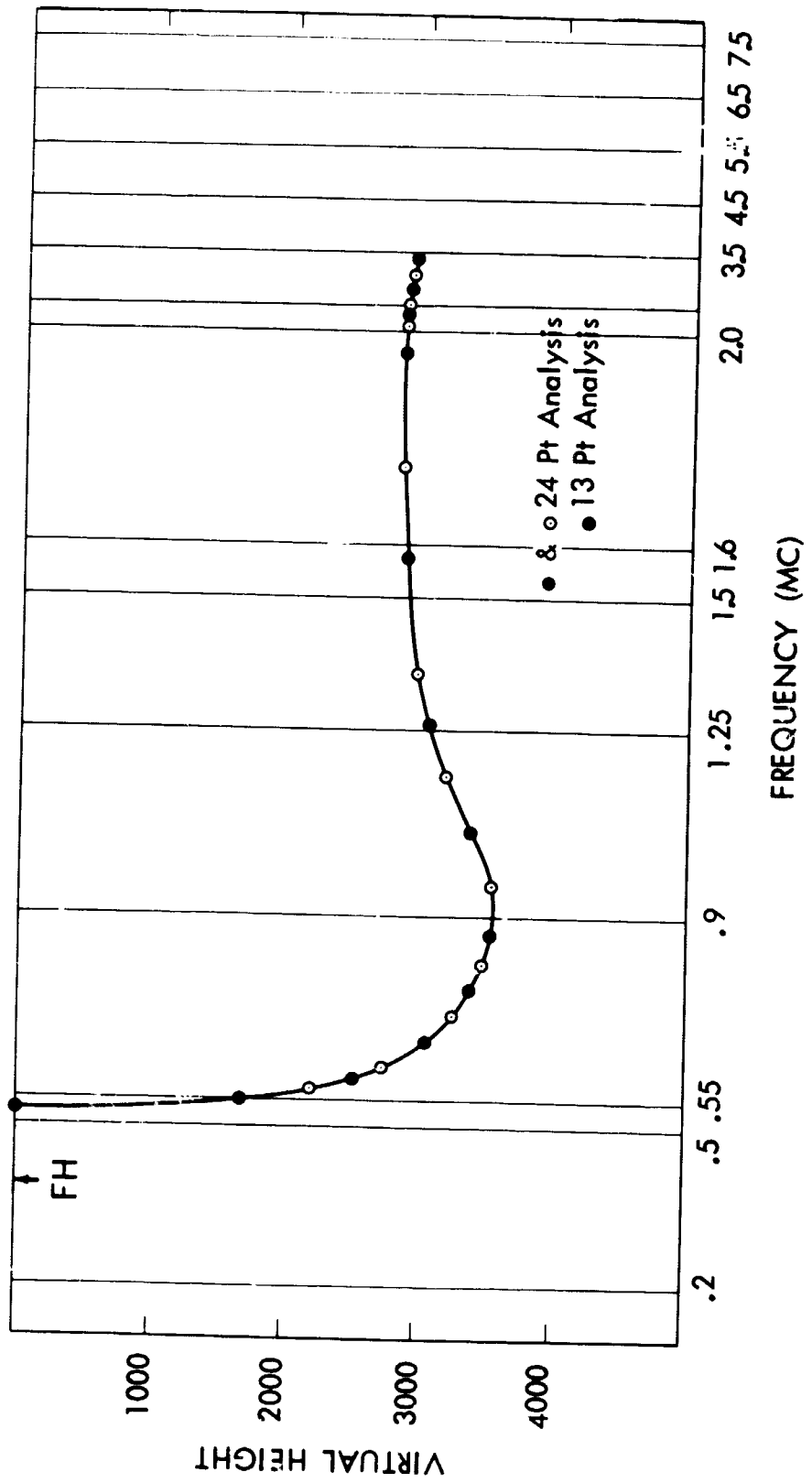
VIRTUAL HEIGHT
1000
2000
3000
4000
FH
.2
.5
.55
.9
1.25
1.5
1.6
2.0
3.5
4.5
5.5
6.5
7.5
FREQUENCY (MC)
● & ○ 24 Pt Analysis
● 13 Pt Analysis

Fig. 8

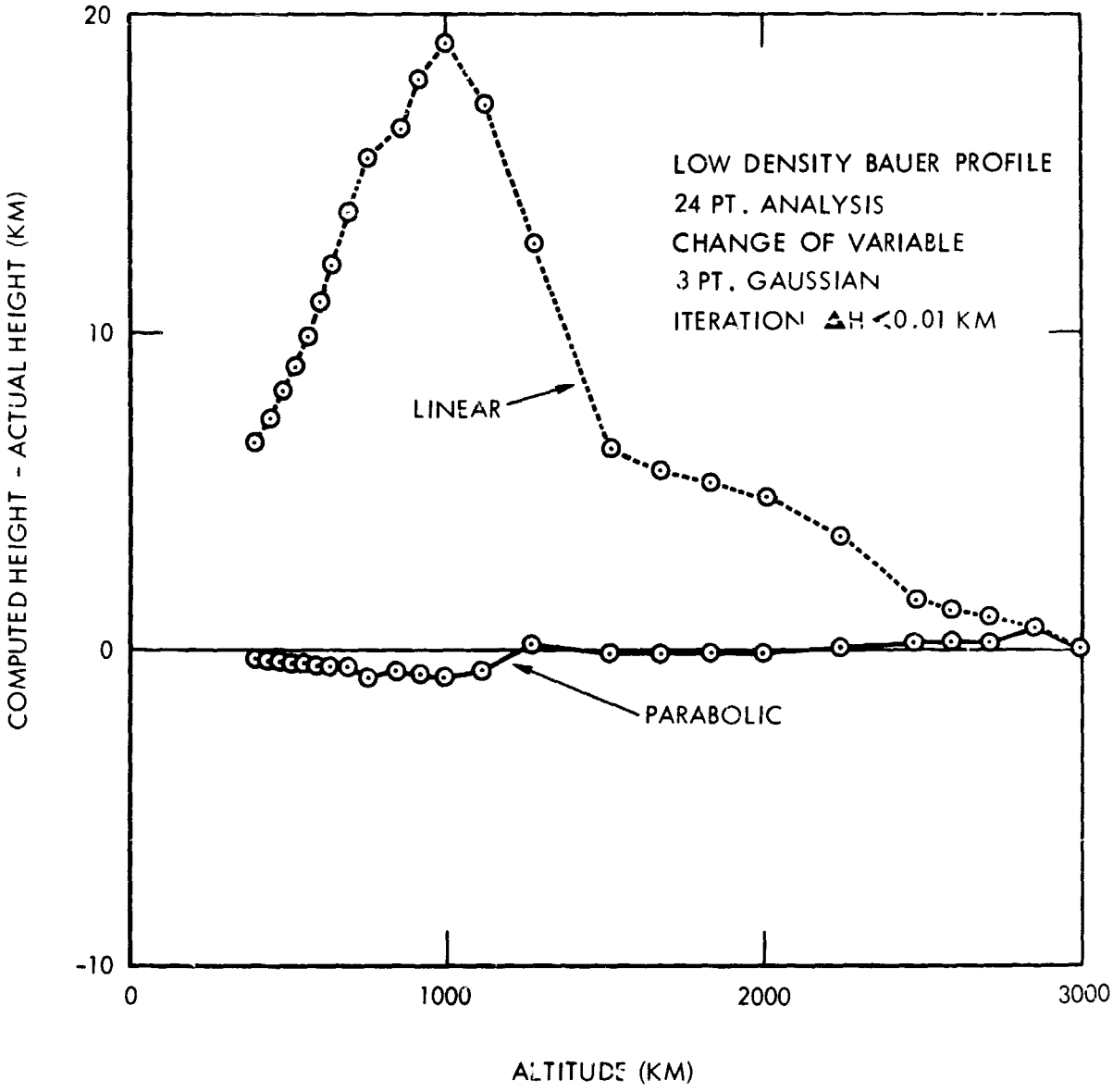
20
10
0
-10
0
1000
2000
3000
COMPUTED HEIGHT - ACTUAL HEIGHT (KM)
ALTITUDE (KM)
LOW DENSITY BAUER PROFILE
24 PT. ANALYSIS
CHANGE OF VARIABLE
3 PT. GAUSSIAN
ITERATION ΔH <0.01 KM
LINEAR
PARABOLIC

Fig. 9

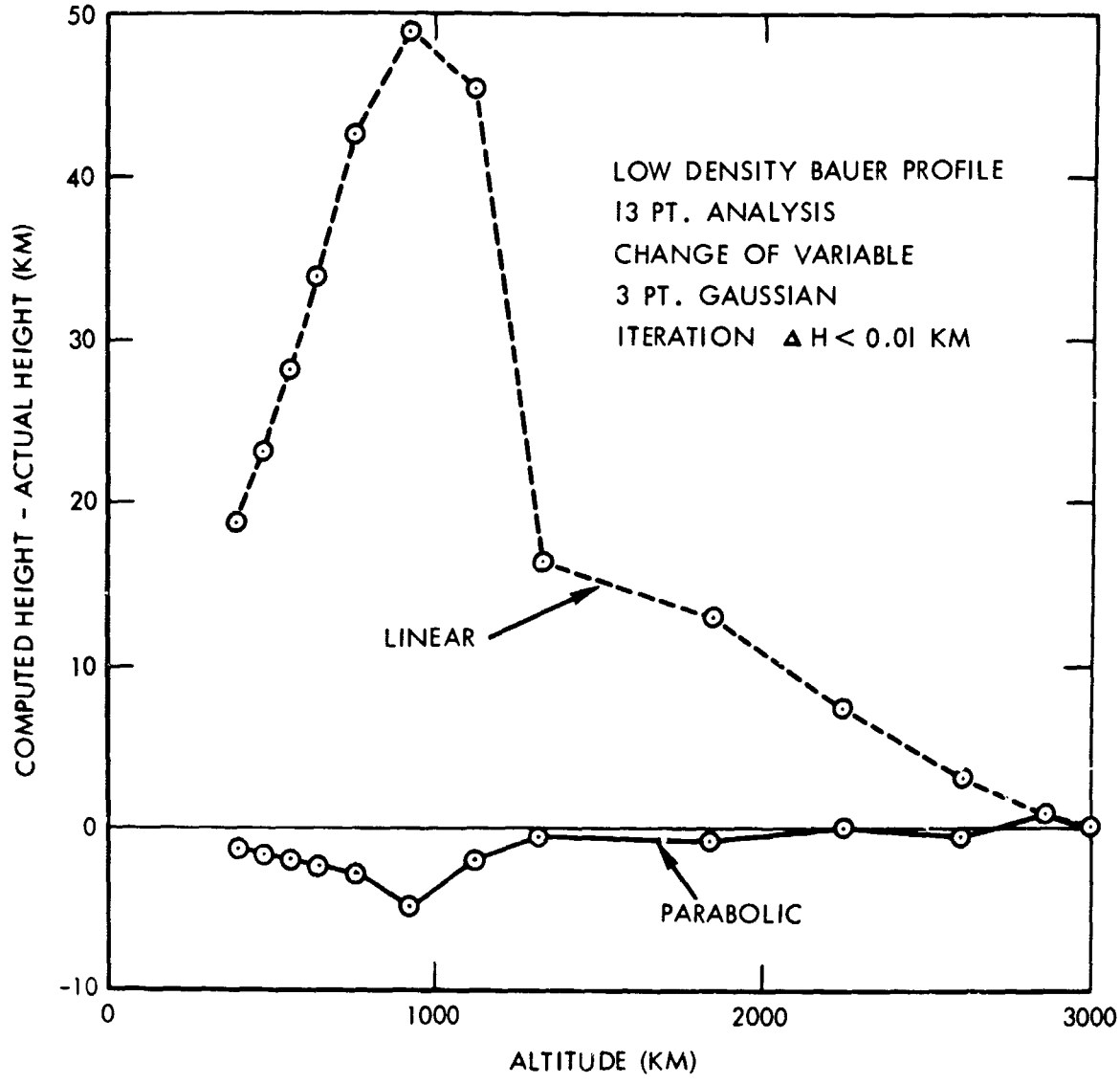
LOW DENSITY BAUER PROFILE
13 PT. ANALYSIS
CHANGE OF VARIABLE
3 PT. GAUSSIAN
ITERATION ΔH < 0.01 KM
LINEAR
PARABOLIC
COMPUTED HEIGHT - ACTUAL HEIGHT (KM)
ALTITUDE (KM)
50
40
30
20
10
0
-10
0
1000
2000
3000

Fig. 10

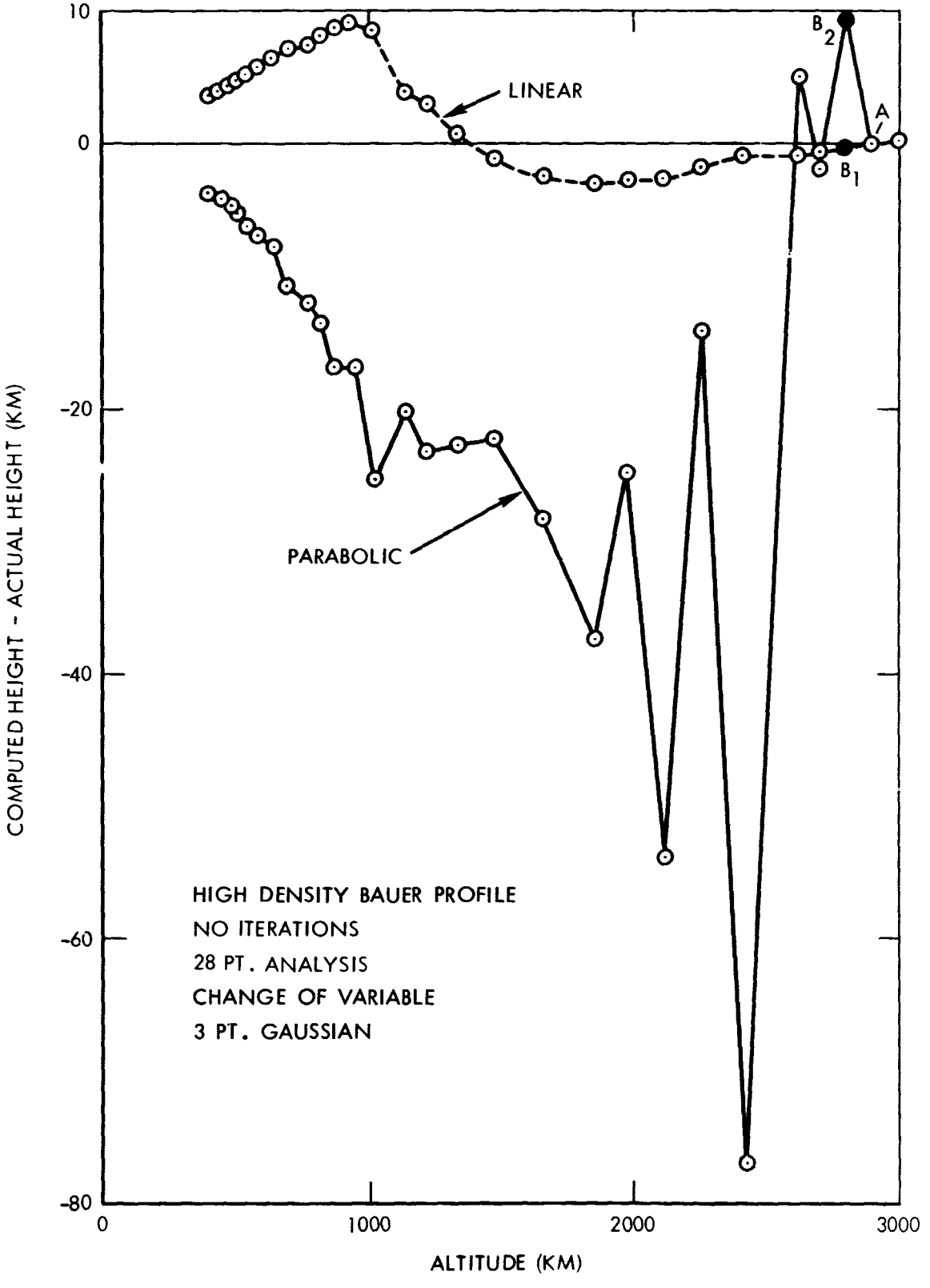
10
0
-20
-40
-60
-80
0
1000
2000
3000
COMPUTED HEIGHT - ACTUAL HEIGHT (KM)
ALTITUDE (KM)
LINEAR
PARABOLIC
A
B2
B1
HIGH DENSITY BAUER PROFILE
NO ITERATIONS
28 PT. ANALYSIS
CHANGE OF VARIABLE
3 PT. GAUSSIAN

Fig. 11

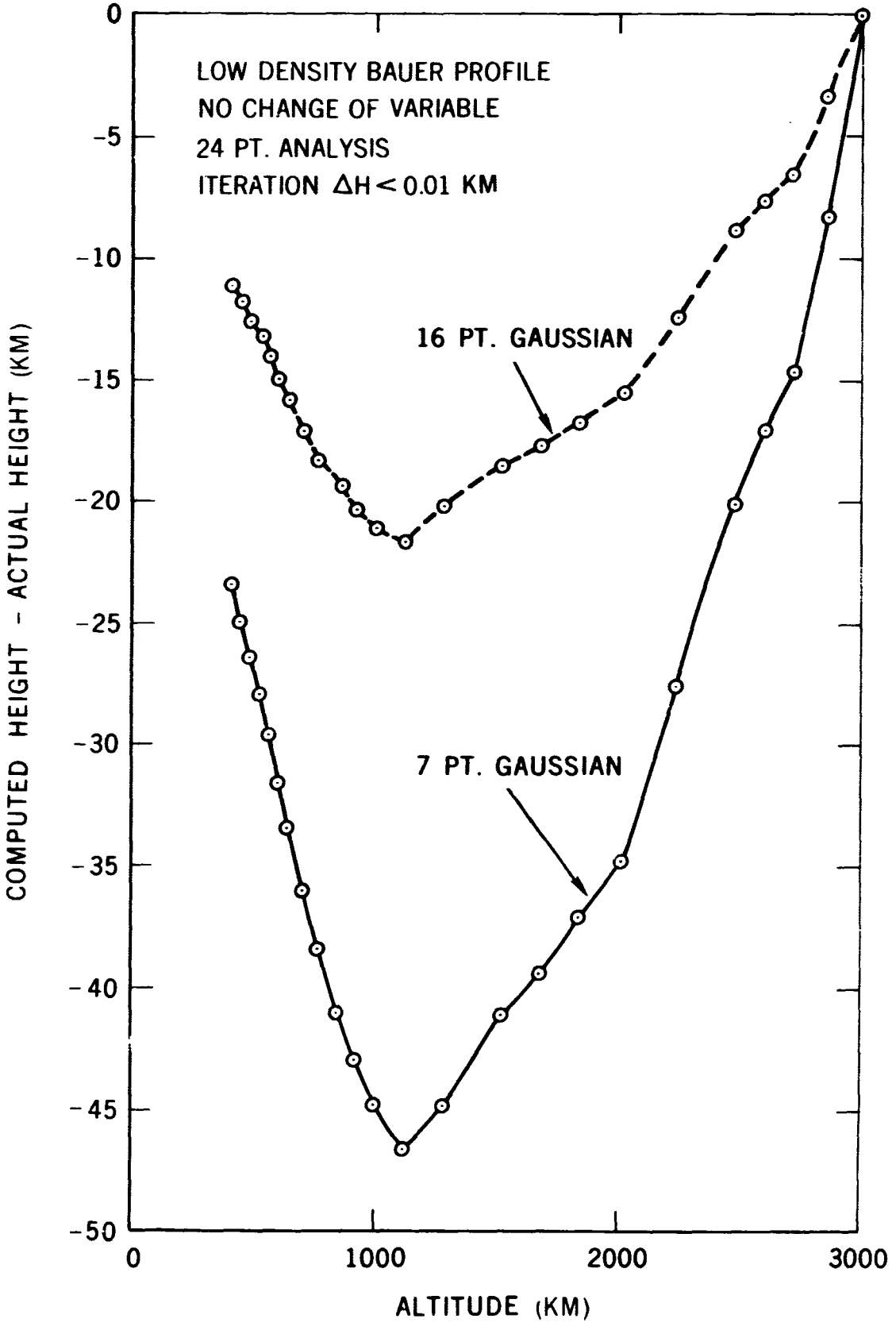
LOW DENSITY BAUER PROFILE
NO CHANGE OF VARIABLE
24 PT. ANALYSIS
ITERATION ΔH < 0.01 KM
16 PT. GAUSSIAN
7 PT. GAUSSIAN
COMPUTED HEIGHT - ACTUAL HEIGHT (KM)
ALTITUDE (KM)
0
-5
-10
-15
-20
-25
-30
-35
-40
-45
-50
0
1000
2000
3000

Fig. 12

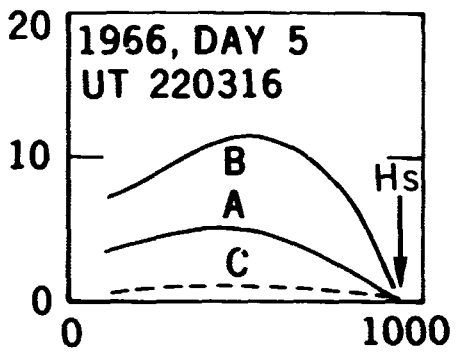

A: 16 PT. GAUSS, 3 ITERATIONS
NO CHANGE IN VARIABLE

B: 7 PT. GAUSS, 3 ITERATIONS
NO CHANGE IN VARIABLE

C: 7 PT. GAUSS, NO ITERATION
CHANGE IN VARIABLE

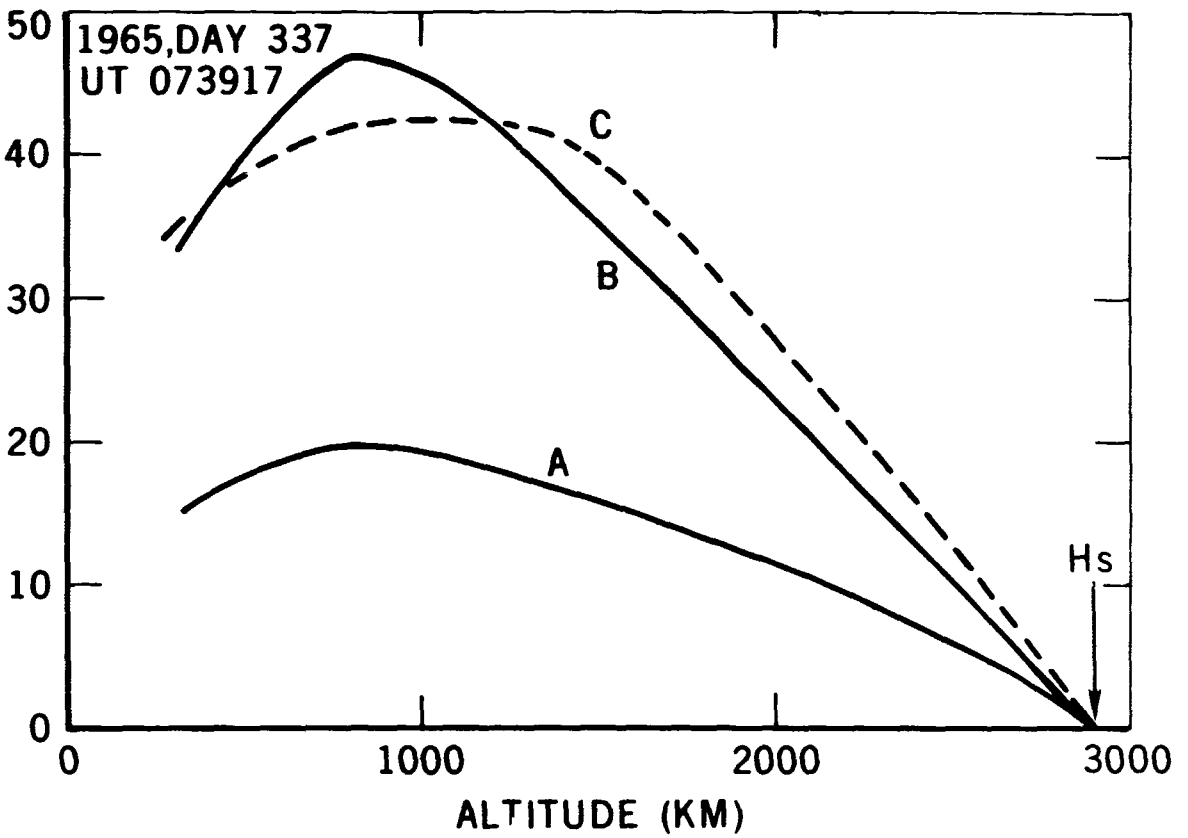

DISTANCE IN KM BELOW CORRECT PROFILE

Fig. B-1

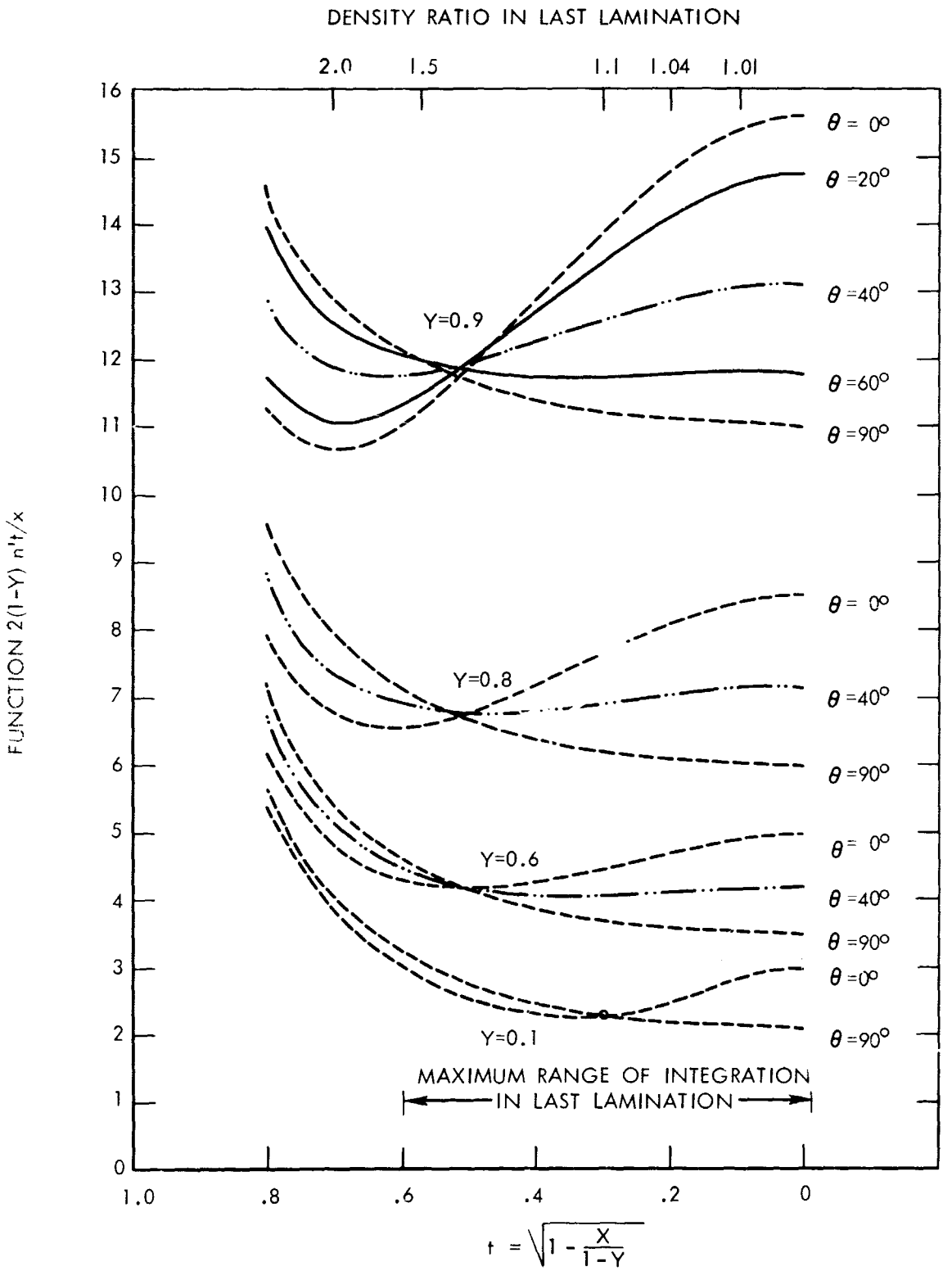
DENSITY RATIO IN LAST LAMINATION
2.0
1.5
1.1
1.04
1.01
FUNCTION 2(1-Y) n't/x
θ = 0°
θ =20°
θ =40°
θ =60°
θ =90°
Y=0.9
θ = 0°
θ =40°
θ =90°
Y=0.8
θ = 0°
θ =40°
θ =90°
Y=0.6
θ =0°
θ =90°
Y=0.1
MAXIMUM RANGE OF INTEGRATION
IN LAST LAMINATION
1.0
.8
.6
.4
.2
0
$t = \sqrt{1 - \frac{X}{1-Y}}$

Fig. B-2

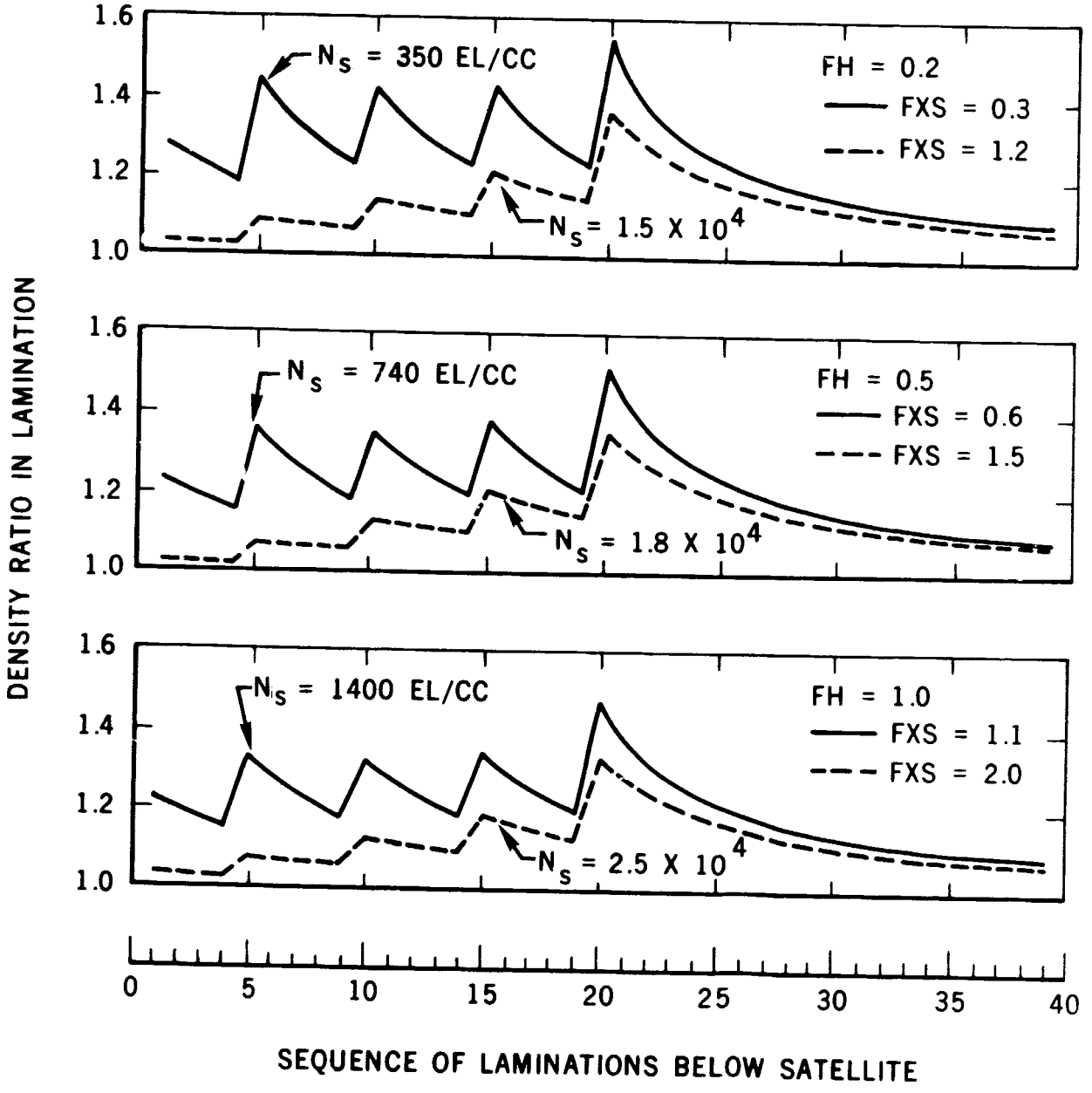
1.6
1.4
1.2
1.0
N_S = 350 EL/CC
FH = 0.2
FXS = 0.3
FXS = 1.2
N_S = 1.5 X 10^4
N_S = 740 EL/CC
FH = 0.5
FXS = 0.6
FXS = 1.5
N_S = 1.8 X 10^4
N_S = 1400 EL/CC
FH = 1.0
FXS = 1.1
FXS = 2.0
N_S = 2.5 X 10^4
DENSITY RATIO IN LAMINATION
0
5
10
15
20
25
30
35
40
SEQUENCE OF LAMINATIONS BELOW SATELLITE

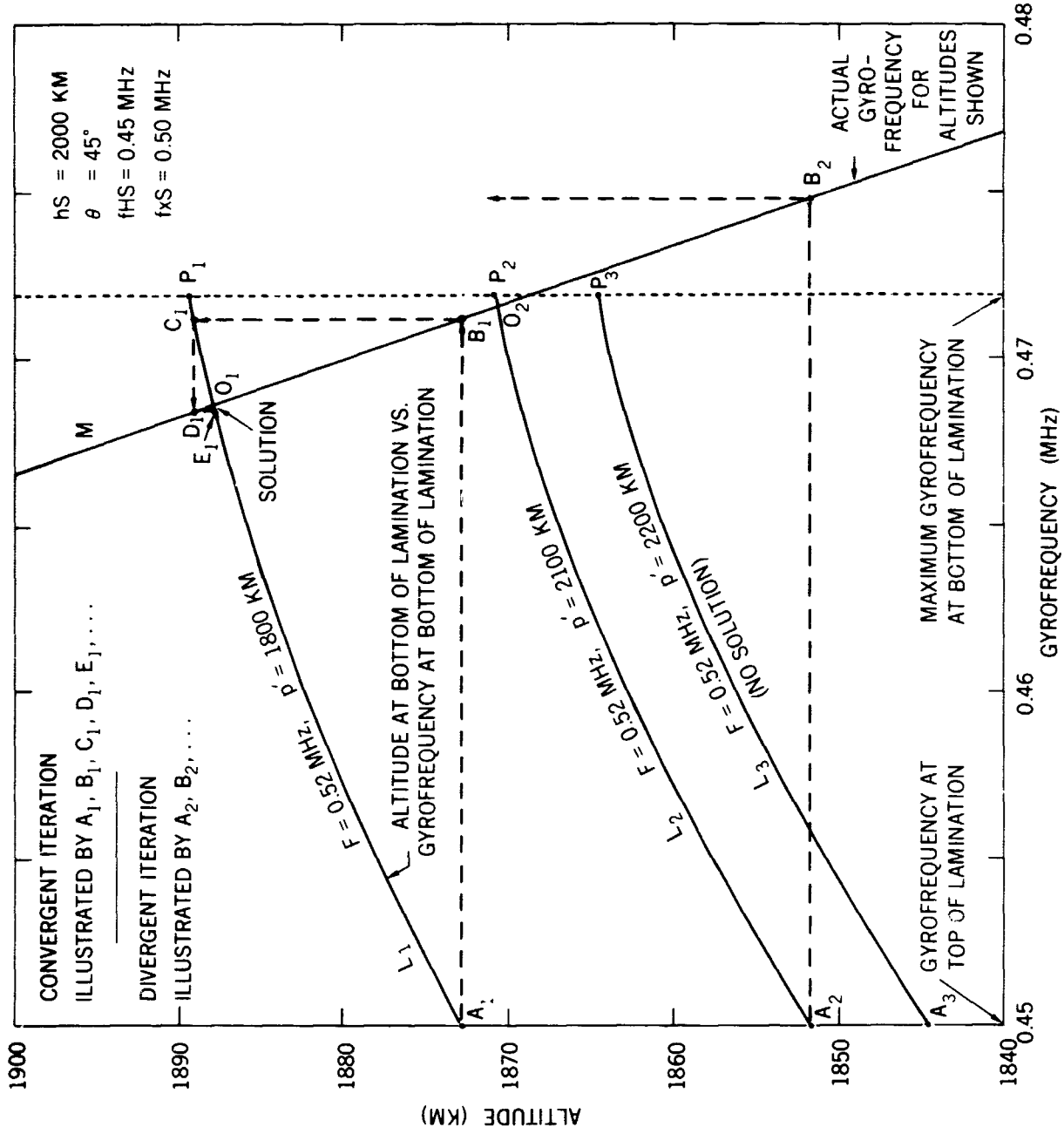
CONVERGENT ITERATION
ILLUSTRATED BY A_1, B_1, C_1, D_1, E_1, ...
DIVERGENT ITERATION
ILLUSTRATED BY A_2, B_2, ...
hS = 2000 KM
θ = 45°
fHS = 0.45 MHz
fxS = 0.50 MHz
M
P_1
C_1
O_1
D_1
E_1
SOLUTION
P_2
B_1
O_2
P_3
B_2
ACTUAL GYRO-FREQUENCY FOR ALTITUDES SHOWN
L_1
F = 0.52 MHz, p' = 1800 KM
ALTITUDE AT BOTTOM OF LAMINATION VS. GYROFREQUENCY AT BOTTOM OF LAMINATION
A_1
L_2
F = 0.52 MHz, p' = 2100 KM
A_2
L_3
F = 0.52 MHz, p' = 2200 KM
(NO SOLUTION)
A_3
GYROFREQUENCY AT TOP OF LAMINATION
MAXIMUM GYROFREQUENCY AT BOTTOM OF LAMINATION
ALTITUDE (KM)
1900
1890
1880
1870
1860
1850
1840
0.45
0.46
0.47
0.48
GYROFREQUENCY (MHz)

Fig. C-1